RESEARCH MEMORANDUM

AERODYNAMIC PERFORMANCE AND STATIC STABILITY AND CONTROL

OF FLAT-TOP HYPERSONIC GLIDERS AT MACH NUMBERS

FROM 0.6 TO 18

By Clarence A. Syvertson, Hermilo R. Gloria,
and Michael F. Sarabia

Ames Aeronautical Laboratory
Moffett Field, Calif.

NATIONAL ADVISORY COMMITTEE
FOR AERONAUTICS
WASHINGTON

September 17, 1958

NACA RM A58G17

NATIONAL ADVISORY COMMITTEE FOR AERONAUTICS

RESEARCH MEMORANDUM

AERODYNAMIC PERFORMANCE AND STATIC STABILITY AND CONTROL

OF FLAT-TOP HYPERSONIC GLIDERS AT MACH NUMBERS

FROM 0.6 TO 18[*]

By Clarence A. Syvertson, Hermilo R. Gloria,
and Michael F. Sarabia

SUMMARY

A study is made of aerodynamic performance and static stability and control at hypersonic speeds. In a first part of the study, the effect of interference lift is investigated by tests of asymmetric models having conical fuselages and arrow plan-form wings. The fuselage of the asymmetric model is located entirely beneath the wing and has a semicircular cross section. The fuselage of the symmetric model was centrally located and has a circular cross section. Results are obtained for Mach numbers from 3 to 12 in part by application of the hypersonic similarity rule. These results show a maximum effect of interference on lift-drag ratio occurring at a Mach number of 5, the Mach number at which the asymmetric model was designed to exploit favorable lift interference. At this Mach number, the asymmetric model is indicated to have a lift-drag ratio 11 percent higher than the symmetric model and 15 percent higher than the asymmetric model when inverted. These differences decrease to a few percent at a Mach number of 12. In the course of this part of the study, the accuracy of the hypersonic similarity rule applied to wing-body combinations is demonstrated with experimental results. These results indicate that the rule may prove useful for determining the aerodynamic characteristics of slender configurations at Mach numbers higher than those for which test equipment is readily available.

In a second part of the study, the aerodynamic performance and static stability and control characteristics of a hypersonic glider are investigated in somewhat greater detail. Results for Mach numbers from 3 to 18 for performance and 0.6 to 12 for stability and control are obtained by standard test techniques, by application of the hypersonic similarity rule, and/or by use of helium as a test medium. Lift-drag ratios of about 5 for Mach numbers up to 18 are shown to be obtainable. The glider

---

[*]Title, Unclassified.

studied is shown to have acceptable longitudinal and directional stability characteristics through the range of Mach numbers studied. Some roll instability (negative effective dihedral) is found at Mach numbers near 12.

INTRODUCTION

Several basic studies have been made of the different types of vehicles suitable for flight at hypersonic speeds. In reference 1, for example, Eggers, Allen, and Neice made a comparative analysis of the performance and heating of ballistic, glide, and skip vehicles, while in references 2, 3, and 4, these vehicles were given further attention. The present investigation is part of the additional study given to hypersonic gliders. Primary attention will be given to aerodynamic performance and static stability and control. Problems associated with aerodynamic heating, propulsion, guidance, etc., are not considered.

Although aerodynamic heating will not be considered in detail, it is recognized at the outset that this problem is very important to the design of a hypersonic glider. It can, in fact, outweigh other usual considerations. For example, aerodynamic heating can make high lift-drag ratios undesirable in some cases, since flight times at conditions of high heating rates can be increased. Usually this situation exists at speeds in the neighborhood of 20,000 feet per second, and for this reason somewhat lower speeds will be considered in the present study. In addition, attention will be restricted to configurations which are at least capable of high aerodynamic performance.

In the selection of configurations to give high lift-drag ratios at hypersonic speeds several schemes have been suggested. For example, in the early work of Sänger (refs. 5 and 6), which was later formalized by Resnikoff (ref. 7), it was deduced theoretically that the optimum lifting arrangement for hypersonic speeds should have a plane or flat-bottom surface. These analyses were based on impact theory for estimates of the pressure forces. The use of impact theory precludes the existence of any interference effects. More recently the use of favorable interference to improve aircraft performance has received wide attention (refs. 8 to 11). In one application (ref. 8), a fuselage consisting of one-half of a body of revolution is mounted entirely beneath an arrow plan-form wing. With this arrangement, the wing experiences favorable lift interference from the pressure field of the fuselage. At Mach numbers up to about 6, it was found that the use of this scheme resulted in increased aerodynamic efficiency.

For Mach numbers greater than about 6, however, it is not clear if similar increases can be realized or if schemes which do not exploit favorable interference, such as use of the flat-bottom arrangement dictated by impact theory, will provide greater efficiency. For this

reason, the effect of interference on aerodynamic efficiency will be considered first in the present study with an investigation of the performance of simple configurations. Detailed consideration will then be given to the aerodynamic characteristics of an example glider.

NOTATION

b span of wing (without tip droop), ft

C_D drag coefficient, $\dfrac{drag}{qS}$

C_L lift coefficient, $\dfrac{lift}{qS}$

C_l rolling-moment coefficient, $\dfrac{rolling\ moment}{qSb}$

C_m pitching-moment coefficient, $\dfrac{pitching\ moment}{qSc}$

C_N normal-force coefficient, $\dfrac{normal\ force}{qS}$

C_n yawing-moment coefficient, $\dfrac{yawing\ moment}{qSb}$

c root chord of wing, ft

g gravitational constant

M free-stream Mach number
      (For definition of equivalent Mach number, see appendix A.)

q free-stream dynamic pressure, lb/sq ft

Re Reynolds number, based on root chord

R_E radius of the earth, $20.9{\times}10^6$ ft

R gas constant

S plan area of wing (without tip droop), sq ft

s range, ft

T temperature, $^{\circ}R$

t maximum thickness of wing, ft

V   velocity, ft/sec

x   length of run, ft

α angle of attack (measured with respect to lower surface of wing for
        asymmetric models), deg

β angle of sideslip, deg

δ_a deflection of left elevon (positive down), deg

δ_E deflection of both elevons (positive down), deg

δ_R deflection of rudder or speed brake (positive trailing edge left
        when viewed from rear), deg

φ roll angle, deg

ρ density, slugs/cu ft

τ shear stress, lb/sq ft

Subscripts

f   skin friction

p   pressure

w   wall conditions

α $\dfrac{\partial}{\partial \alpha}$

β $\dfrac{\partial}{\partial \beta}$

δ outer edge of boundary layer

EXPERIMENT

Models

The models employed in the study of the effect of aerodynamic
interference on performance are shown in figure 1. The asymmetric model
(fig. 1(a)) had a fuselage formed from one-half of a cone of fineness
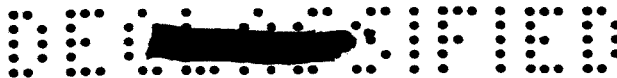
ratio 5. To the flat top of this body was mounted a wing of arrow plan form having a leading-edge sweep of 77.4°. The wing had an aspect ratio of 1.43 and a total length apex to tip of 1.4 times the root chord. The wing section was a simple wedge 2 percent thick in streamwise planes and 9.2 percent thick in planes normal to the leading edge. The apex of the wing and the tip of the fuselage were coincident and the fuselage length was equal to the wing root chord. The symmetric model (fig. 1(b)) had the same plan form, wing and body base area, and wing and body volume as the asymmetric model. To satisfy these conditions, the body diameter for the symmetric model was smaller than for the asymmetric model.

These models were tested at Mach numbers from 3 to 6 with the asymmetric model tested in both upright and inverted attitudes. To provide data for higher Mach numbers, use was made of the hypersonic similarity rule (appendix A). To implement the use of this rule, the hypersonically similar models shown in figure 2 were also tested. These models differ from those shown in figure 1 only in that the thickness and span to chord ratios are doubled.

A scale model and a hypersonically similar model of a glider are shown in figure 3. Details of the glider design will be discussed later in the text.

Apparatus and Tests

The experimental investigation was conducted in the Ames 10- by 14-inch supersonic wind tunnel (ref. 12) and in the Ames 2- by 2-foot transonic wind tunnel (ref. 13). Tests were conducted in the 2- by 2-foot wind tunnel at Mach numbers from 0.6 to 1.3, angles of attack from -2° to +15°, and angles of sideslip from -8° to +2°. Tests were conducted in the 10- by 14-inch wind tunnel at Mach numbers from 3.0 to 6.0, angles of attack from -2° to +11°, and angles of sideslip from -4° to +4°. Additional tests at Mach numbers of 9 and 12 were conducted using helium as the test medium. Reynolds numbers for the tests are shown below:

M	Re/ft, (million)
0.6 - 1.3	4.20
3	9.14
4	8.87
5	3.83
6	2.15
9	4.15
12	6.21

Aerodynamic forces and moments were measured by strain-gage balances. Each model was supported from the rear by the strain-gage balance assembly which was shrouded to within 0.04 inch of the model base thereby eliminating, for all practical purposes, any aerodynamic loads on the support system. Base pressures were measured in all tests and the resultant base forces (referred to free-stream static pressure) were subtracted from the measured axial forces.

Precision of the experimental results is affected by uncertainties in the measured forces, moments, and base pressure, as well as in the determination of free-stream static and dynamic pressures and angle of attack. Variations in free-stream Mach number did not exceed ±0.05 at Mach numbers from 0.6 to 6 and ±0.3 at Mach numbers 9 and 12. Variations in free-stream Reynolds number did not exceed ±20,000 from values given previously. The estimated error in angle of attack and control deflection did not exceed ±0.2°. The combination of these uncertainties resulted in possible errors in the aerodynamic force and moment coefficients as given in the following table:

Mach number	C_L, C_N	C_D	C_m	C_Y	C_l	C_n
0.6 to 1.3	±0.002	- - -	±0.001	±0.0005	±0.00005	±0.0005
3 to 5	±.002	±0.0005	±.001	±.0005	±.00005	±.0005
6	±.004	±.0008	±.002	±.001	±.0001	±.001
9 and 12	±.008	±.0012	±.004	±.002	±.0002	±.002

It should be noted that, for the most part, the experimental results presented herein are in error by less than these estimates.

RESULTS AND DISCUSSION

Basic Configurations

In the initial part of this investigation, an attempt was made to evaluate at hypersonic speeds the effect of aerodynamic interference on performance by study of simple models. Since accurate well-established theories for the estimate of wing-body aerodynamic characteristics at hypersonic speeds are virtually nonexistent,[1] this study was based on

---

[1] Recently, Savin (ref. 14) has developed an approximate theory applicable to configurations of the type suggested in reference 8. This theory is not applicable to configurations which have all or part of the fuselage located on the lee side of the wing, and therefore it could not be used in the present study.

experimental results. The models used in this investigation are shown in figure 1. The asymmetric model was tested in both upright and inverted attitudes. In its upright attitude the asymmetric model is a wing-body combination which exploits favorable lift interference. Its design Mach number is 5 according to the principles given in reference 8. At this Mach number, the wing leading edge coincides with the body shock wave and thus the wing just contains the interference pressure field of the body. In its inverted attitude, the asymmetric model represents a flat-bottom configuration as dictated by impact theory. The particular model was, however, designed to exploit favorable interference and thus does not necessarily represent an ideal flat-bottom configuration. For this reason, comparison of the aerodynamic performance of configurations upright and inverted will provide primarily a qualitative measure of the effect of interference. These models were tested at Mach numbers from 3 to 6. To obtain data for higher Mach numbers, use was made of the hypersonic similarity rule as described in appendix A. The hypersonically similar models corresponding to the study configurations are shown in figure 2. All of the data obtained in the tests of these models are presented in table I for reference purposes. Only a summary of these results will be considered in detail.

Since part of the results were obtained through application of the hypersonic similarity rule, the accuracy of this rule must first be established. As noted in appendix A, transformation of the data obtained with the similar models is straightforward with the possible exception of the drag coefficients. In this case, corrections must be applied for the friction drag since the similarity rules apply only to pressure forces. To this end, the friction-drag coefficient for test conditions, estimated as described in appendix B, was subtracted from the experimentally determined total-drag coefficient. The remainder, the pressure drag, was transformed with the similarity rule. To this transformed drag coefficient was added the friction-drag coefficient for a set of assumed flight conditions, estimated as also described in appendix B. This procedure was adopted in order to put the results obtained with and without the aid of the hypersonic similarity rule on a common basis. Flight conditions were deemed to be most representative for this purpose. For the flight conditions a transition Reynolds number of 3 million was assumed and it was also assumed that the configurations were gliders and thus base drag for the fuselage, which is not contained in the test results (table I), was added. In all cases, it was assumed that the base-pressure coefficient was 70 percent of the vacuum value.

Drag coefficients obtained in this manner are shown in figure 4 for the asymmetric model at zero angle of attack. Data for Mach numbers less than 6 were obtained with the scale model; data for Mach numbers greater than 6 were obtained from tests of the similar model at one-half the Mach number shown. For this reason the abscissa is labeled "equivalent Mach number." Estimated drag coefficients are also shown. To obtain these estimates, the fuselage pressure drag was obtained from reference 15;

the wing pressure drag, from linear theory assuming two-dimensional flow; the wing leading-edge drag, from impact theory; and the friction and base drag, as previously discussed. In general, the agreement between the estimated and experimentally derived results is good. At a Mach number of 6, there is some difference between the results obtained with the scale and the similar models, but the two results show about the same difference from the estimated drag curve.

Another demonstration of the accuracy of the similarity rule is shown in figure 5 where the lift curve and lift-drag polar for the asymmetric model at a Mach number of 6 are presented. In this figure, data obtained both from tests of the scale model at a Mach number of 6 and from tests of the similar model at a Mach number of 3 are shown. The two sets of results show good agreement. At an angle of attack of 5°, for example, the two values of lift coefficient differ by less than 10 percent and the two values of drag coefficient differ by about 6 percent.

With these results to demonstrate the accuracy of the similarity rule, results obtained with the rule for Mach numbers up to 12 will now be examined. In figure 6, maximum lift-drag ratios for the symmetric model and for the asymmetric model in both upright and inverted attitudes are shown as a function of Mach number. Again the drag results have been adjusted to the assumed flight conditions. At a Mach number of 6, where results were obtained with and without the aid of the hypersonic similarity rule, the difference between corresponding points is 2 percent or less.

There are several trends worth noting in the results shown in figure 6. First, the effect of interference (i.e., the effect of wing-fuselage arrangement) on performance is largest at Mach numbers near 5. At this Mach number in particular, the lift-drag ratio obtained with the upright asymmetric model is 11 percent higher than that obtained with the symmetric model and 15 percent higher than that obtained with the inverted asymmetric model. At least in part, this maximum difference occurs at a Mach number of 5 because this is the design Mach number of the upright asymmetric model (ref. 8); at this Mach number the model is designed to take maximum advantage of favorable lift interference. At higher Mach numbers the effect of wing-fuselage arrangement decreases. At a Mach number of 12, the highest for which results are shown, the effect of fuselage location is small, of the order of a few percent.

In view of the results shown in figure 6 it would appear worthwhile to examine the effect of changes in the design Mach number of the asymmetric model. Some indication of this effect can be obtained again with the aid of the hypersonic similarity rule. If only the data for the asymmetric model at the design Mach number of 5 are used, these data can be transformed with the rule to any other Mach number. These transformed data would represent the characteristics of another similar model, but always at its design Mach number. Results obtained in this manner are

shown in figure 7 along with sketches of several of the configurations. Due to the transformation, they become increasingly slender with increasing Mach number. In particular, the fuselage fineness ratios are numerically equal to the Mach numbers. These results, when compared to those shown in figure 6, show a somewhat greater effect of interference at the higher Mach numbers; however, the effect still decreases with increasing Mach number. At least in part, the differences between these results and those shown in figure 6 are associated with the extreme slenderness of the configurations in figure 7 at the higher Mach numbers.

While all of these results show a decreasing effect of wing-fuselage arrangement at hypersonic speeds, the asymmetric model tested upright did, in general, yield the highest performance of the arrangements studied and, in fact, at lower speeds showed an appreciable advantage. This finding must again be tempered, however, with the fact that the particular asymmetric model tested was designed to exploit the advantages of favorable lift interference. The possibility certainly exists that more efficient designs of other types could be found. In addition, since aerodynamic performance is only one of the factors which influences the design of hypersonic gliders, the choice of wing-fuselage arrangement may be dictated by other factors at the higher Mach numbers. Thus all three arrangements tested warrant further investigation at hypersonic speeds; however, the remainder of this study is restricted to a more thorough investigation of the aerodynamic characteristics of an example hypersonic glider designed for favorable lift interference.

Hypersonic Glider

Configuration.- The glider studied is shown in figure 8. This configuration was selected for study purposes to bring to light problems associated with flight of hypersonic gliders. Although an attempt was made to make the glider a practical design, it should not be considered as an actual airplane. The dimensions shown in figure 8 are for a full-scale vehicle which could, if so desired, be man-carrying. The fuselage is 65.2 feet long and is formed from half of a minimum-drag body of revolution (ref. 16). The estimated weight was 21,500 pounds excluding fuel, and the center of gravity was estimated to be at 76 percent of the wing root chord aft of the nose and 2.7 percent of the root chord beneath the lower surface of the wing.

The wing has a modified arrow plan form with rectangular tips to provide control surfaces. The wing leading edges are swept back 77.4°, the wing root chord is 58 feet, the wing span is 32.5 feet, and the total plan-form area is 1075 square feet (for the wing with tips horizontal). The aspect ratio is 1 and the wing loading is 20 pounds per square foot. From considerations of aerodynamic heating, the apex of the wing and the nose of the fuselage are blunted to form the surface of a hemisphere with

a radius of 2 inches. Similarly, the wing leading edge has a diameter
of 3/8 inch except near the tips where the diameter is 5-1/2 inches.
The wing section is a simple wedge with a maximum thickness of 12.5 inches
and blunt trailing edges.

To provide directional stability, the wing tips have a droop of 45°
about a line toed in 3° with respect to the plane of symmetry. To aug-
ment directional stability, a ventral fin is provided. This fin is con-
sidered to be extended at Mach numbers less than 6 and retracted at higher
speeds. Longitudinal and lateral control are provided by plain trailing-
edge flaps at the wing tips. Directional control at Mach numbers below 6
is provided by a rudder on the ventral fin. At higher speeds, directional
control is provided by body flaps at the base of the fuselage. These
flaps could also function as dive brakes.

A model of this glider at approximately 1/100-scale and a hyperson-
ically similar model with thickness and span to chord ratios doubled
(see fig. 3) were tested in the same manner as the models discussed pre-
viously. Both models were also tested in helium. The scale model was
tested at a nominal Mach number of 12, and the similar model at a Mach
number of 9 to provide data for a Mach number of 18. All of the test
results obtained are presented in tables II and III. Only a summary of
these results will be considered in detail. Longitudinal data are pre-
sented in terms of wind axes while lateral data are presented in terms
of body axes.

Performance.- Some of the results relative to the performance of
the glider are shown in figure 9, where lift curves and lift-drag polars
for Mach numbers of 6 and 12 are presented. Pitching-moment coefficients
are also shown. The drag has been corrected to assumed flight conditions
as described in appendix B, again assuming a transition Reynolds number
of 3 million. For a Mach number of 6, data obtained with both the scale
and similar model tested in air are shown. The agreement is about the
same as was found for the basic models. For a Mach number of 12, data
obtained with the similar model tested in air at a Mach number of 6 and
the scale model tested in helium are shown. With the exception of the
pitching-moment data, these two sets of results are also in good agree-
ment. The differences in the two sets of pitching-moment data are due,
at least in part, to scatter or inaccuracies in the data obtained in
helium. While these differences are large, they amount to a difference
in aerodynamic center of only about 2 percent of root chord.

From these and other results the maximum trimmed lift-drag ratios
for the glider were obtained and these values are shown in figure 10.
Results are shown for Mach numbers from 3 to 18. At Mach numbers less
than 6, the flag on the symbol indicates the ventral fin is extended.
As will be discussed later in consideration of stability and control,
the glider is essentially self-trimming at supersonic speeds, and for
this reason, trim drag has an almost negligible effect on the lift-drag

DECLASSIFIED

ratios shown in figure 10. Although the results shown were obtained from four different types of tests, the over-all variation of lift-drag ratio with Mach number appears consistent. The highest lift-drag ratio of 5.7 occurs at a Mach number of 6. However, it decreases to about 4.7 at a Mach number of 3 and 4.8 at a Mach number of 18. The decrease at lower Mach numbers is associated with the increased contribution of base drag. The decrease at higher Mach numbers is associated in part with an increased drag due to lift and in part with the increase in the percentage of drag due to skin friction.

From these lift-drag ratios, the range capability of the glider has been estimated from numerical integration of the equation

$$\frac{ds}{R_E} = \left(\frac{L}{D}\right) \frac{V \, dV}{gR_E - V^2}$$

With this equation only the conversion of kinetic energy of velocity into range is considered; the potential energy of altitude is neglected. The results of the calculations are presented in figure 11. These results indicate that the glider is capable of a range of about 2250 nautical miles with an initial glide velocity of 12,000 feet per second or about 5740 nautical miles with an initial velocity of 18,000 feet per second. In the first case, the mean lift-drag ratio (i.e., the constant value of lift-drag ratio required to get the same range with the same initial velocity) is about 5.4, and in the second case, about 5.1.

Static stability and control.- Typical results showing the longitudinal characteristics of the glider are presented in figure 12 where normal-force coefficient is shown as a function of angle of attack and pitching-moment coefficient. Results are shown for Mach numbers of 0.6, 1.3, 5, and 12 and control deflections of -20°, 0°, and +20°. These deflections are for one control only since in the tests only the left elevon was deflected. For a Mach number of 0.6, the stability characteristics are somewhat nonlinear and at the higher normal-force coefficients longitudinal instability is indicated. At a Mach number of 1.3, the situation is somewhat improved, and there is an increase in stability through the entire range of normal-force coefficients. At a Mach number of 5, the characteristics are approximately linear, at least to an angle of attack of about 7°. At this Mach number, and more so at a Mach number of 12, the effectiveness of the control is greater when it is deflected in the windward direction (positive deflections) than when it is deflected toward the lee side of the wing. This effect, which is typical of hypersonic speeds, becomes more pronounced at the higher angles of attack.

The longitudinal-stability characteristics are summarized in figure 13 where the static longitudinal stability for 5° angle of attack and the elevator deflection estimated for trim at this attitude are shown

as a function of Mach number. This angle of attack is close to that for maximum lift-drag ratio, and hence the results shown in figure 13 are indicative of the characteristics of the glider in cruise flight. In general, these results show that the longitudinal stability is almost constant at supersonic speeds with a static margin of about 0.05. At transonic and subsonic speeds there is a loss in stability but at a Mach number of 0.6, the glider is still at least marginally stable. Elevator deflections required for trim are small at supersonic speeds. Thus the glider is essentially self-trimming and trim-drag penalties were found to be negligible. Further indication of the control effectiveness is shown in figure 14, where the ratio $\Delta C_m/\Delta \delta_e$ is shown as a function of Mach number again for 5° angle of attack. The incremental ratio rather than the usual derivative is shown since few control deflections were tested. Ratios for both positive and negative control deflections are shown. In general, these results show that the control maintains its effectiveness throughout the range of test Mach numbers, although the control characteristics are nonlinear at the higher Mach numbers.

The directional and lateral stability of the glider are shown in figures 15 and 16 where the parameters C_{n_β} and C_{l_β} are shown as a function of Mach number for angles of attack of 0°, 3°, and 7°. For Mach numbers from 0.6 to 6, results are shown for the ventral fin extended, and for Mach numbers from 3 to 12, for the fin retracted. In general, these results show that if the ventral fin is kept extended at Mach numbers less than about 6, the configuration is directionally stable throughout the range of test variables. The parameter, C_{l_β} (fig. 16), is sometimes positive, however, indicating negative effective dihedral, particularly at the lower angles of attack. At lower Mach numbers, the term, C_{l_β}, becomes negative with increasing angle of attack. This effect of angle of attack decreases with increasing Mach number, however, and at the higher Mach numbers the positive values of C_{l_β} persist to angles of attack corresponding to cruise conditions.

Limited data defining the lateral and directional control characteristics are presented in figure 17 for an angle of attack of 5°. Since the elevons are located on the drooped wing tips, their differential deflection as ailerons produces yawing as well as rolling moments. As the results in figure 17 show, these yawing moments are of the same magnitude as, and even larger than, the rolling moments produced by the ailerons. The rudder effectiveness shown at Mach numbers up to 6 is for the rudder on the ventral fin. This control also produces appreciable rolling moments. At a Mach number of 12, the rudder effectiveness is for the body-flap control. This control produced but small rolling moments.

The foregoing study of the lateral and directional stability and control characteristics was not extensive. It did, however, bring to light certain problems associated with configurations of the type studied.

For example, a very brief analog-simulation study was made of the flight characteristics of the glider at a Mach number of 12. This study indicated stability augmentation was required to overcome the negative effective dihedral. When this augmentation was supplied by the ailerons, the yawing moments produced by these controls caused directional instability. Only if both the ailerons and the body-flap controls were employed in combination, did lateral and directional stability result. It is apparent, therefore, that additional studies of the lateral and directional stability and control problems would be required before the characteristics could be considered entirely satisfactory.

CONCLUDING REMARKS

In a first part of the present study, the effect of aerodynamic interference on performance of hypersonic gliders at Mach numbers from 3 to 12 was investigated by tests of asymmetric and symmetric models having arrow plan-form wings and conical fuselages. The results of this investigation indicated that the maximum effect of wing-fuselage arrangement on lift-drag ratio occurred at a Mach number of 5, the Mach number at which the asymmetric model was designed to exploit favorable lift interference. At this Mach number the asymmetric model with fuselage entirely beneath the wing had a lift-drag ratio 11 percent higher than the symmetric model and 15 percent higher than the asymmetric model when inverted. These differences decreased with increasing Mach number and were the order of a few percent at a Mach number of 12. In the course of the investigation, the accuracy of the hypersonic similarity rule applied to wing-body combinations was demonstrated with experimental results, and it was indicated that this rule may prove useful for determining the aerodynamic characteristics of slender wing-body combinations at Mach numbers higher than those for which test equipment is readily available.

In a second part of the present investigation, the aerodynamic performance and static stability and control characteristics of a hypersonic glider designed for favorable lift interference were studied in somewhat greater detail at Mach numbers from 0.6 to 18. The results indicated that lift-drag ratios of about 5 are obtainable for Mach numbers up to 18. The glider studied had acceptable longitudinal and directional stability characteristics through the range of Mach numbers covered. Some roll instability (negative effective dihedral) was indicated at Mach numbers near 12. This problem will require further study.

Ames Aeronautical Laboratory
    National Advisory Committee for Aeronautics
        Moffett Field, Calif., July 17, 1958

APPENDIX A

HYPERSONIC SIMILARITY RULE

The similarity rule for hypersonic flow was first introduced by Tsien (ref. 17) and is now well treated in the literature (see, e.g., refs. 17 to 19). With the aid of the rule, the aerodynamic character- istics of a series of slender configurations can be related approximately, provided the shapes of the configurations are related by an affine trans- formation and provided the similarity parameters

$$\left.\begin{aligned}
K_t &= M(t/c) \\
K_b &= M(b/c) \\
K_\alpha &= M\alpha \\
K_\beta &= M\beta \\
K_\varphi &= \varphi
\end{aligned}\right\} \tag{A1}$$

are the same for each configuration. If these conditions are satisfied, then the various force and moment coefficients can be correlated by

$$\left.\begin{aligned}
(M^2 C_L)_1 &= (M^2 C_L)_2 \\
(M^3 C_{D_p})_1 &= (M^3 C_{D_p})_2 \\
(M^2 C_m)_1 &= (M^2 C_m)_2 \\
(M^2 C_Y)_1 &= (M^2 C_Y)_2 \\
(M C_n)_1 &= (M C_n)_2 \\
(M^2 C_l)_1 &= (M^2 C_l)_2
\end{aligned}\right\} \tag{A2}$$

where the subscripts 1 and 2 refer to two configurations which have the same values of similarity parameters, equations (A1). The correlation equations (A2) are for coefficients referenced to plan area. If coef- ficients were based on base or cross-section area, the exponent of Mach number would be reduced by 1 in each of the relations. In addition, it

should be noted that the rule applies only to pressure forces and thus
values of the drag coefficient used in the correlations must not contain
skin friction.

The present application of the rule was relatively straightforward.
A model of the configuration for which results were desired was con-
structed with thickness and span to chord ratios doubled. This config-
uration was tested at a given Mach number and angles of attack, sideslip,
and roll to obtain a given set of similarity parameters (A1) and corre-
lated coefficients (A2). These results were used to determine the char-
acteristics for the original configuration at equivalent conditions of
twice the Mach number, one-half the angles of attack and sideslip, and
at the same roll angle.

NACA RM A58G17

APPENDIX B

SKIN-FRICTION DRAG

As noted previously, the hypersonic similarity rule does not apply for the friction drag. The friction drag for test conditions and for assumed flight conditions were estimated. The purpose of this appendix is to describe how these estimates were made.

Test Conditions

The basic method used to estimate the skin friction for test conditions was the T' method of Rubesin and Johnson (ref. 20) as modified by Sommer and Short (ref. 21). With this method, the friction-drag coefficient was estimated by integrating the following expression over the wetted surface of the models:

$$C_{D_f} = \frac{1}{Sq} \int \tau \, ds \qquad (B1)$$

where

$$\tau = C_f' \rho' \frac{V_\delta^2}{2} \qquad (B2)$$

and

$$\rho' = \frac{p_\delta}{RT'} \qquad (B3)$$

In addition, C_f', the friction coefficient, is evaluated for a Reynolds number

$$Re' = \rho' \frac{V_\delta x}{\mu'} \qquad (B4)$$

where x is the length of run and where μ' is the viscosity evaluated at T'. For laminar flow, the friction coefficient was calculated with

$$C_f' = \frac{0.664}{\sqrt{Re'}} \tag{B5}$$

and with

$$T' = T_\delta \left[1 + 0.032\, M_\delta^2 + 0.58 \left(\frac{T_w}{T_\delta} - 1\right)\right] \tag{B6}$$

If an adiabatic wall and a recovery factor of 0.85 are assumed, this expression becomes for air,

$$T' = T_\delta \left(1 + 0.131\, M_\delta^2\right) \tag{B7}$$

With the same assumptions, only the numerical constant changes for helium; hence,

$$T' = T_\delta \left(1 + 0.218\, M_\delta^2\right) \tag{B8}$$

For turbulent flow, the expressions are

$$C_f' = \frac{0.0576}{(Re')^{1/5}} \tag{B9}$$

and

$$T' = T_\delta \left[1 + 0.035\, M_\delta^2 + 0.45 \left(\frac{T_w}{T_\delta} - 1\right)\right] \tag{B10}$$

If an adiabatic wall and a recovery factor of 0.89 are assumed for air

$$T' = T_\delta \left(1 + 0.115\, M_\delta^2\right) \tag{B11}$$

The character of the boundary layer was observed with the aid of shadowgraphs. At test Mach numbers of 3 and 4, it was observed to be essentially all turbulent and accordingly all turbulent flow was assumed. At a test Mach number of 5, the flow was transitional and the location of transition was observed for each model. On the average, however, about half of the model surface had laminar flow and half, turbulent. In the evaluation of turbulent friction downstream of transition, the

length of run was assumed to start at the leading edge and thus no
detailed correction for transition was made. At a test Mach number of 6,
the flow was observed to be all laminar. At test Mach numbers of 9 and 12
in helium, the shadowgraph lacked sufficient sensitivity to define the
character of the flow. At these Mach numbers, all laminar flow was
assumed.

For laminar flow at Mach numbers of 5, 6, 9, and 12, the effect of
boundary-layer displacement on skin friction can not be neglected
(ref. 22). For these cases, a correction was applied for this effect
as is described in detail by Bertram in appendix C of reference 23.

Flight Conditions

The above approximations were employed to estimate skin friction
for assumed flight conditions. To obtain the altitude and hence the
free-stream conditions, it was assumed that the configurations had a
wing loading of 20 pounds per square foot. The fuselages were assumed
to be 50 feet long. It was first assumed the configurations were at an
angle of attack of 4° and friction drag was evaluated. The lift coef-
ficient for maximum lift-drag ratio then was evaluated and a single iter-
ation was performed to correct friction drag. In the evaluation of the
wall temperature in equations (B6) and (B10), radiation equilibrium tem-
perature was used except where it exceeded 1800° F. If this value was
exceeded, then it was assumed that the skin would be cooled to this tem-
perature. For flight conditions, transition was assumed to occur at a
length Reynolds number of 3 million. It is possible that for the high
degree of leading-edge sweep of the present test models, this assumed
transition Reynolds number is somewhat optimistic. In addition, flight
Reynolds numbers were sufficiently high that no correction for the
boundary-layer displacement effect was made.

DECLASSIFIED

REFERENCES

1. Eggers, A. J., Jr., Allen, H. Julian, and Neice, Stanford E.:   A Comparative Analysis of the Performance of Long-Range Hypervelocity Vehicles.   NACA TN 4046, 1957.

2. Allen, H. Julian, and Eggers, A. J., Jr.:   A Study of the Motion and Aerodynamic Heating of Missiles Entering the Earth's Atmosphere at High Supersonic Speeds.   NACA TN 4047, 1957.

3. Seiff, Alvin, and Allen, H. Julian: Some Aspects of the Design of Hypersonic Boost-Glide Aircraft.   NACA RM A55E26, 1955.

4. Ferri, Antonio, Feldman, Lewis, and Daskin, Walter: The Use of Lift for Re-entry from Satellite Trajectories.   Jet Propulsion, vol. 27, no. 11, Nov. 1957, pp. 1184-1191.

5. Sänger, Eugen: Raketen-flugtechnik.   R. Oldenbourg (Berlin), 1933, pp. 112, 120-121.

6. Sänger, E., and Bredt, I.:   A Rocket Drive for Long Range Bombers. Bur. Aero., Navy Dept. Trans. CGD-32, 1944, pp. 58-64.

7. Resnikoff, Meyer M.:   Optimum Lifting Bodies at High Supersonic Air Speeds.   NACA RM A54B15, 1954.

8. Eggers, A. J., Jr., and Syvertson, Clarence A.:   Aircraft Configurations Developing High Lift-Drag Ratios at High Supersonic Speeds. NACA RM A55L05, 1956.

9. Ferri, Antonio, Clarke, Joseph H., and Casaccio, Anthony: Drag Reduction in Lifting Systems by Advantageous Use of Interference. PIBAL Rep. 272, Polytechnic Institute of Brooklyn, Dept. Aero. Eng. and Appl. Mech., May 1955.

10. Rossow, Vernon J.:   A Theoretical Study of the Lifting Efficiency at Supersonic Speeds of Wing Utilizing Indirect Lift Induced by Vertical Surfaces.   NACA RM A55L08, 1956.

11. Syvertson, Clarence A., Wong, Thomas J., and Gloria, Hermilo R.: Additional Experiments With Flat-Top Wing-Body Combinations at High Supersonic Speeds.   NACA RM A56I11, 1957.

12. Eggers, A. J., Jr., and Nothwang, George J.:   The Ames 10- by 14-Inch Supersonic Wind Tunnel.   NACA TN 3095, 1954.

13. Spiegel, Joseph M., and Lawrence, Leslie F.: A Description of the Ames 2- by 2-Foot Transonic Wind Tunnel and Preliminary Evaluation of Wall Interference. NACA RM A55I21, 1956.

14. Savin, Raymond C.: Approximate Solutions for the Flow About Flat-Top Wing-Body Configurations at High Supersonic Airspeeds. NACA RM A58F02, 1958.

15. Staff of the Computing Section (under the direction of Zdeněk Kopal): Tables of Supersonic Flow Around Cones. Tech. Rep. 1, Center of Analysis, M.I.T., Cambridge, 1947.

16. Eggers, A. J., Jr., Resnikoff, Meyer M., and Dennis, David H.: Bodies of Revolution Having Minimum Drag at High Supersonic Airspeeds. NACA Rep. 1306, 1957. (Supersedes NACA TN 3666)

17. Tsien, Hsue-shen: Similarity Laws of Hypersonic Flows. Jour. Math. and Phys., vol. 25, no. 3, Oct. 1946, pp. 247-251.

18. Hayes, Wallace D.: On Hypersonic Similitude. Quart. Appl. Math., vol. V, no. 1, Apr. 1947, pp. 105-106.

19. Hamaker, Frank M., Neice, Stanford E., and Wong, Thomas J.: The Similarity Law for Hypersonic Flow and Requirements for Dynamic Similarity of Related Bodies in Free Flight. NACA Rep. 1147, 1953. (Supersedes NACA TN's 2443 and 2631)

20. Rubesin, M. W., and Johnson, H. A.: A Critical Review of Skin-Friction and Heat-Transfer Solutions of the Laminar Boundary Layer of a Flat Plate. Trans. A.S.M.E., vol. 71, no. 4, May 1949, pp. 383-388.

21. Sommer, Simon C., and Short, Barbara J. Free-Flight Measurements of Turbulent-Boundary-Layer Skin Friction in the Presence of Severe Aerodynamic Heating at Mach Numbers From 2.8 to 7.0. NACA TN 3391, 1955.

22. Lees, Lester, and Probstein, Ronald F.: Hypersonic Viscous Flow over a Flat Plate. Rep. No. 195, Princeton Univ., Aero. Eng. Lab., Apr. 20, 1952.

23. Bertram, Mitchel H.: Boundary-Layer Displacement Effects in Air at Mach Numbers of 6.8 and 9.6. NACA TN 4133, 1958.

TABLE I.- PERFORMANCE DATA FOR ASYMMETRIC AND SYMMETRIC MODELS
(a) Scale asymmetric model

M	Re, millions	α, deg	c_L	c_D	M	Re, millions	α, deg	c_L	c_D
3	6.1	-7.5	-0.1267	0.0243	5	2.6	-7.2	-0.0948	0.0173
		-6.4	-.1067	.0197			-6.2	-.0795	.0139
		-5.3	-.0854	.0159			-5.1	-.0643	.0111
		-4.2	-.0630	.0128			-4.1	-.0495	.0089
		-3.1	-.0404	.0105			-3.1	-.0341	.0072
		-2.1	-.0185	.0091			-2.0	-.0184	.0066
		-1.0	.0075	.0086			-1.0	-.0021	.0060
		.1	.0288	.0085			0	.0183	.0063
		1.2	.0506	.0101			1.1	.0354	.0070
		2.3	.0673	.0120			2.1	.0520	.0083
		3.3	.0895	.0148			3.1	.0692	.0103
		4.4	.1116	.0186			4.2	.0840	.0129
		5.5	.1316	.0228			5.2	.0984	.0164
		6.6	.1523	.0282			6.2	.1131	.0205
		7.7	.1714	.0341					
4	5.8	-7.5	-.1046	.0199	6	1.4	-7.1	-.0821	.0155
		-6.4	-.0882	.0163			-6.1	-.0690	.0130
		-5.3	-.0734	.0135			-5.1	-.0561	.0104
		-4.3	-.0555	.0109			-4.0	-.0425	.0088
		-3.2	-.0371	.0090			-3.0	-.0297	.0076
		-2.1	-.0183	.0078			-2.0	-.0173	.0071
		-1.0	.0021	.0075			-1.0	-.0006	.0068
		.1	.0219	.0075			0	.0126	.0065
		1.2	.0409	.0085			1.0	.0296	.0071
		2.3	.0604	.0103			2.0	.0433	.0082
		3.4	.0792	.0128			3.1	.0587	.0100
		4.5	.0960	.0160			4.1	.0719	.0122
		5.5	.1133	.0201			5.1	.0854	.0152
		6.6	.1287	.0245			6.1	.0981	.0186
		7.7	.1450	.0298			7.1	.1117	.0227

TABLE I.- PERFORMANCE DATA FOR ASYMMETRIC AND SYMMETRIC MODELS - Continued
(b) Hypersonically similar asymmetric model

M	Re, millions	α, deg	C_L	C_D	M	Re, millions	α, deg	C_L	C_D
3	4.3	-11.8	-0.2474	0.0662	5	1.8	-10.3	-0.1678	0.0479
		-10.7	-.2228	.0571			-9.3	-.1468	.0409
		-9.6	-.1977	.0487			-8.2	-.1248	.0346
		-8.5	-.1722	.0415			-7.2	-.1034	.0295
		-7.5	-.1475	.0351			-6.1	-.0828	.0254
		-6.4	-.1249	.0308			-5.1	-.0620	.0219
		-5.3	-.0954	.0261			-4.1	-.0416	.0196
		-4.2	-.0672	.0228			-3.0	-.0180	.0187
		-3.1	-.0379	.0203			-2.0	.0038	.0175
		-2.0	-.0089	.0181			-1.0	.0256	.0177
		-.8	.0285	.0180			.1	.0477	.0191
		.4	.0652	.0199			1.1	.0690	.0214
		1.6	.0991	.0230			2.2	.0905	.0247
		2.8	.1325	.0276			3.2	.1119	.0287
		3.5	.1547	.0308			4.2	.1297	.0332
		4.0	.1833	.0377			5.3	.1491	.0389
		5.7	.2102	.0452			6.3	.1711	.0450
		6.8	.2376	.0543			7.4	.1928	.0518
		7.9	.2627	.0639			8.4	.2188	.0621
		9.0	.2877	.0748			9.4	.2385	.0713
		10.1	.3092	.0861					
		11.2	.3319	.0986	6	1.0	-11.1	-.1651	.0504
		12.2	.3527	.1118			-10.1	-.1452	.0433
							-9.1	-.1253	.0369
4	4.2	-10.8	-.1915	.0511			-8.1	-.1055	.0317
		-9.7	-.1700	.0437			-7.1	-.0869	.0274
		-8.6	-.1483	.0373			-6.1	-.0683	.0243
		-7.5	-.1266	.0318			-5.0	-.0510	.0218
		-6.4	-.1025	.0256			-4.0	-.0335	.0200
		-5.3	-.0794	.0220			-3.0	-.0134	.0192
		-4.2	-.0567	.0191			-2.0	.0011	.0191
		-3.1	-.0303	.0177			-1.0	.0190	.0197
		-2.0	-.0047	.0166			0	.0370	.0205
		-.9	.0218	.0171			1.1	.0553	.0224
		.2	.0478	.0180			2.1	.0732	.0249
		1.3	.0735	.0204			3.1	.0915	.0276
		2.4	.0995	.0241			4.1	.1098	.0310
		3.5	.1237	.0284			5.1	.1290	.0348
		4.6	.1427	.0337			6.1	.1465	.0399
		5.7	.1681	.0411			7.2	.1642	.0464
		6.8	.1940	.0493			8.2	.1831	.0538
		7.9	.2188	.0585			9.2	.2042	.0625
		9.1	.2423	.0687			10.2	.2255	.0726
		10.1	.2635	.0791			11.2	.2470	.0837
		11.2	.2820	.0898					

TABLE I.- PERFORMANCE DATA FOR ASYMMETRIC AND SYMMETRIC MODELS - Continued
(c) Scale symmetric model

M	Re, millions	α, deg	c_L	c_D	M	Re, millions	α, deg	c_L	c_D
3	6.1	-1.1	-0.0213	0.0104	5	2.6	-1.0	-0.0170	0.0072
		0	.0001	.0097			0	-.0001	.0067
		1.1	.0215	.0102			1.0	.0177	.0069
		2.3	.0431	.0114			2.1	.0336	.0078
		3.5	.0656	.0137			3.1	.0492	.0094
		4.6	.0875	.0169			4.1	.0641	.0115
		5.8	.1090	.0211			5.2	.0795	.0143
		6.9	.1299	.0260			6.2	.0941	.0176
							7.2	.1090	.0215
4	5.8	-1.1	-.0202	.0084					
		0	-.0001	.0078	6	1.4	-1.0	-.0135	.0076
		1.1	.0200	.0083			0	.0005	.0069
		2.2	.0386	.0094			1.0	.0148	.0069
		3.3	.0568	.0113			2.0	.0287	.0077
		4.4	.0747	.0139			3.0	.0409	.0092
		5.4	.0901	.0170			4.1	.0542	.0108
		6.5	.1071	.0210			5.1	.0674	.0132
		7.6	.1231	.0254			6.1	.0809	.0161
							7.1	.0935	.0194

TABLE I.- PERFORMANCE DATA FOR ASYMMETRIC AND SYMMETRIC MODELS - Concluded

(d) Hypersonically similar symmetric model

M	Re, millions	α, deg	C_L	C_D	M	Re, millions	α, deg	C_L	C_D
3	4.3	-1.1	-0.0341	0.0227	5	1.8	-1.0	-0.0200	0.0172
		0	-.0005	.0216			0	.0004	.0170
		1.1	.0336	.0224			1.0	.0205	.0172
		2.2	.0671	.0249			2.1	.0408	.0187
		3.3	.0989	.0284			3.1	.0710	.0209
		4.4	.1280	.0331			4.2	.0912	.0246
		5.5	.1611	.0390			5.2	.1122	.0290
		6.6	.1873	.0458			6.2	.1337	.0343
		7.7	.2139	.0540			7.3	.1557	.0406
		8.8	.2405	.0632			8.3	.1779	.0481
		9.9	.2658	.0731			9.4	.2035	.0570
		11.0	.2906	.0841			10.4	.2277	.0668
		12.0	.3155	.0963	6	1.0	-1.0	-.0203	.0188
4	4.2	-1.1	-.0256	.0190			0	-.0005	.0185
		0	-.0004	.0185			1.0	.0200	.0187
		1.1	.0275	.0189			2.0	.0402	.0194
		2.2	.0535	.0207			3.0	.0613	.0210
		3.3	.0804	.0238			4.1	.0807	.0230
		4.4	.1065	.0280			5.1	.0998	.0270
		5.5	.1313	.0330			6.1	.1191	.0320
		6.6	.1562	.0394			7.1	.1397	.0381
		7.7	.1807	.0468			8.1	.1599	.0448
		8.8	.2043	.0550			9.2	.1806	.0520
		9.9	.2265	.0641			10.2	.2019	.0604
		11.0	.2488	.0741					

DECLASSIFIED

TABLE II.- PERFORMANCE DATA FOR GLIDER
(a) Scale model with ventral fin

M	Re, millions	α, deg	C_L	C_D	M	Re, millions	α, deg	C_L	C_D
3	5.3	-2.1	-0.0230	0.0106	5	2.3	-2.0	-0.0172	0.0070
		-1.0	-.0029	.0097			-1.0	-.0014	.0066
		.2	.0175	.0096			0	.0150	.0067
		1.3	.0389	.0104			1.1	.0301	.0073
		2.4	.0633	.0121			2.1	.0458	.0085
		3.0	.0752	.0133			2.6	.0530	.0094
		3.6	.0873	.0147			3.1	.0606	.0104
		4.2	.0995	.0165			3.6	.0681	.0117
		4.7	.1116	.0185			4.2	.0753	.0130
		5.8	.1309	.0227			5.2	.0950	.0167
		7.0	.1525	.0283			6.2	.1101	.0206
							7.2	.1260	.0253
4	5.2	-2.1	-.0197	.0086			8.3	.1414	.0304
		-1.0	-.0016	.0079			9.3	.1571	.0364
		.1	.0156	.0077			9.8	.1729	.0413
		1.2	.0332	.0084					
		2.2	.0518	.0098	6	1.3	-2.0	-.0146	.0079
		2.8	.0611	.0107			-1.0	-.0011	.0073
		3.3	.0703	.0118			0	.0121	.0075
		3.9	.0793	.0132			1.0	.0256	.0082
		4.4	.0891	.0148			2.0	.0394	.0095
		5.5	.1053	.0181			3.0	.0526	.0111
		6.6	.1222	.0223			3.6	.0595	.0123
		7.6	.1397	.0274			4.1	.0660	.0135
		8.7	.1569	.0333			5.1	.0777	.0166
		9.8	.1727	.0395			6.1	.0909	.0200
		10.4	.1900	.0451			7.1	.1055	.0240
							8.1	.1208	.0289
							9.1	.1360	.0342
							9.7	.1519	.0390

TABLE II.- PERFORMANCE DATA FOR GLIDER - Continued
(b) Scale model without ventral fin

M	Re, millions	α, deg	C_L	C_D	M	Re, millions	α, deg	C_L	C_D
3	5.3	-2.1	-0.0237	0.0100	5	2.3	2.6	0.0518	0.0086
		-1.0	-.0043	.0091			3.1	.0592	.0097
		.1	.0165	.0091			3.6	.0668	.0110
		1.3	.0380	.0100			4.2	.0741	.0123
		2.4	.0609	.0116			5.2	.0868	.0147
		3.0	.0730	.0129			6.2	.1024	.0186
		3.6	.0852	.0144			7.2	.1177	.0228
		4.2	.0974	.0162			8.3	.1330	.0279
		4.7	.1093	.0182			9.3	.1486	.0336
		5.9	.1297	.0221			10.3	.1644	.0399
		7.0	.1519	.0277					
		8.2	.1731	.0344	6	1.3	-2.0	-.0142	.0074
		8.7	.1835	.0378			-1.0	-.0011	.0071
							0	.0114	.0072
4	5.2	-2.0	-.0200	.0080			1.0	.0251	.0079
		-1.0	-.0035	.0074			2.0	.0389	.0092
		.1	.0147	.0072			3.0	.0530	.0108
		1.2	.0325	.0079			3.6	.0598	.0119
		2.2	.0509	.0092			4.1	.0663	.0131
		3.3	.0695	.0113			5.1	.0802	.0162
		4.4	.0868	.0141			6.1	.0938	.0197
		5.5	.1036	.0175			7.1	.1089	.0237
		6.6	.1204	.0217			8.1	.1233	.0284
		7.6	.1377	.0267			9.1	.1381	.0340
		8.7	.1555	.0326			10.2	.1540	.0401
		9.8	.1722	.0390					
		10.9	.1890	.0462	12	3.7	1.0	.0109	.0061
							2.1	.0208	.0067
5	2.3	-2.0	-.0193	.0063			3.1	.0308	.0081
		-1.0	-.0042	.0059			4.1	.0390	.0096
		0	.0131	.0059			5.1	.0469	.0118
		1.1	.0289	.0066			6.1	.0550	.0149
		2.1	.0441	.0077			7.1	.0740	.0198

TABLE II.- PERFORMANCE DATA FOR GLIDER - Concluded
(c) Hypersonically similar model without ventral fin

M	Re, millions	α, deg	C_L	C_D	M	Re, millions	α, deg	C_L	C_D
3	3.8	-2.0	-0.0122	0.0220	5	1.6	3.1	0.0767	0.0234
		-.8	.0172	.0210			4.2	.0958	.0268
		.3	.0464	.0212			5.2	.1170	.0316
		1.4	.0750	.0227			6.2	.1372	.0367
		2.6	.1054	.0254			7.2	.1571	.0427
		3.7	.1343	.0285			8.3	.1771	.0494
		4.8	.1634	.0346			9.3	.1982	.0573
		6.0	.1897	.0410			10.3	.2184	.0656
		7.1	.2179	.0480					
		8.2	.2455	.0570	6	.9	-2.0	-.0168	.0165
		9.3	.2728	.0670			-1.0	-.0005	.0164
							0	.0144	.0169
4	3.7	-2.0	-.0161	.0194			1.0	.0299	.0180
		-.9	.0065	.0188			2.0	.0464	.0200
		.2	.0292	.0189			3.1	.0635	.0225
		1.2	.0523	.0201			4.1	.0812	.0256
		2.3	.0757	.0223			5.1	.0996	.0294
		3.4	.0980	.0251			6.1	.1171	.0344
		4.5	.1222	.0292			7.1	.1361	.0400
		5.6	.1469	.0347			8.1	.1554	.0465
		6.6	.1695	.0404			9.1	.1752	.0533
		7.7	.1936	.0474			10.2	.1952	.0608
		8.8	.2145	.0549					
		9.8	.2363	.0634	9	1.7	-2.0	.0032	.0184
		10.9	.2599	.0736			0	.0099	.0186
							1.0	.0132	.0200
5	1.6	-2.0	-.0145	.0176			2.1	.0255	.0227
		-1.0	.0025	.0173			3.2	.0401	.0259
		0	.0215	.0177			5.1	.1006	.0324
		1.1	.0395	.0189			7.1	.1189	.0408
		2.1	.0598	.0209			9.2	.1722	.0601
							10.2	.2070	.0729

TABLE III.- STATIC STABILITY AND CONTROL CHARACTERISTICS OF GLIDER

M	Re, millions	δ_a, deg	δ_r, deg	α, deg	C_N	C_m	C_Y	C_n	C_l
0.6	2.5	0	0	-1.0	-0.0262	0.0082	0.0035	-0.0008	-0.0006
				0	-.0039	.0073	.0035	-.0004	-.0005
				1.1	.0191	.0072	.0035	.0001	-.0006
				2.1	.0448	.0071	.0042	.0001	-.0008
				3.2	.0748	.0076	.0057	-.0004	-.0010
				5.4	.1462	.0064	.0065	.0004	-.0011
				7.6	.2238	.0080	.0048	.0033	-.0014
				9.8	.3068	.0088	.0100	.0013	-.0031
				11.9	.3881	.0109	.0133	0	-.0038
		-20	0	-1.0	-.0510	.0219	.0221	-.0202	-.0094
				0	-.0302	.0210	.0218	-.0194	-.0092
				1.0	-.0082	.0207	.0212	-.0181	-.0090
				2.1	.0171	.0206	.0208	-.0172	-.0087
				3.1	.0475	.0201	.0210	-.0164	-.0084
				5.3	.1214	.0175	.0210	-.0142	-.0075
				7.4	.1970	.0179	.0214	-.0122	-.0077
				9.6	.2764	.0209	.0241	-.0127	-.0091
				11.7	.3579	.0266	.0266	-.0127	-.0105
		20	0	-1.0	-.0052	-.0023	-.0138	.0118	.0068
				0	.0172	-.0029	-.0143	.0125	.0072
				1.1	.0394	-.0030	-.0149	.0131	.0072
				2.1	.0637	-.0024	-.0148	.0133	.0071
				3.2	.0963	-.0035	-.0151	.0139	.0070
				5.3	.1671	-.0040	-.0149	.0146	.0070
				7.4	.2479	-.0039	-.0161	.0169	.0073
				9.6	.3317	-.0028	-.0163	.0183	.0074
				11.7	.4084	.0001	-.0164	.0197	.0071
		0	30	-1.0	-.0244	.0072	-.0309	.0139	.0020
				0	-.0032	.0068	-.0303	.0140	.0020
				1.1	.0184	.0075	-.0301	.0143	.0022
				2.1	.0451	.0067	-.0296	.0146	.0020
				3.1	.0725	.0070	-.0288	.0146	.0017
				5.3	.1425	.0061	-.0274	.0137	.0013
				7.4	.2199	.0063	-.0272	.0172	.0009
				9.5	.2894	.0091	-.0230	.0155	-.0006
				11.7	.3811	.0124	-.0193	.0142	-.0013

TABLE III.- STATIC STABILITY AND CONTROL CHARACTERISTICS OF GLIDER - Continued

M	Re, millions	δ_a, deg	δ_r, deg	α, deg	C_N	C_m	C_Y	C_n	C_l
0.9	2.5	0	0	-1.0	-0.0266	0.0087	0.0030	-0.0006	-0.0005
				0	-.0031	.0079	.0025	.0002	-.0006
				1.1	.0202	.0076	.0040	-.0005	-.0006
				2.2	.0478	.0078	.0040	.0003	-.0007
				3.3	.0809	.0072	.0049	.0004	-.0009
				5.5	.1566	.0054	.0057	.0013	-.0009
				7.8	.2405	.0042	.0048	.0040	-.0013
				9.9	.3240	.0046	.0091	.0023	-.0031
		-20	0	-1.1	-.0530	.0227	.0233	-.0225	-.0094
				0	-.0287	.0214	.0229	-.0216	-.0092
				1.1	-.0048	.0208	.0233	-.0208	-.0091
				2.1	.0211	.0210	.0232	-.0201	-.0090
				3.2	.0530	.0204	.0224	-.0184	-.0087
				5.4	.1291	.0162	.0214	-.0153	-.0075
				7.6	.2100	.0162	.0229	-.0140	-.0080
				9.8	.2924	.0184	.0269	-.0156	-.0101
				10.9	.3342	.0193	.0281	-.0159	-.0110
		20	0	-1.0	-.0066	-.0016	-.0145	.0120	.0069
				0	.0160	-.0025	-.0149	.0125	.0073
				1.1	.0401	-.0031	-.0149	.0127	.0073
				2.2	.0674	-.0030	-.0150	.0130	.0072
				3.2	.1004	-.0039	-.0147	.0133	.0069
				5.4	.1746	-.0058	-.0146	.0142	.0075
				7.6	.2564	-.0069	-.0158	.0163	.0077
				9.8	.3401	-.0066	-.0159	.0177	.0075
				11.9	.4263	-.0062	-.0178	.0207	.0084
		0	30	-1.0	-.0209	-.0073	-.0308	.0148	.0021
				0	.0014	.0063	-.0306	.0151	.0020
				1.1	.0239	.0066	-.0302	.0154	.0022
				2.1	.0517	.0064	-.0297	.0156	.0021
				3.2	.0833	.0058	-.0288	.0157	.0016
				5.4	.1563	.0040	-.0281	.0166	.0014
				7.5	.2385	.0025	-.0286	.0191	.0014
				9.8	.3300	.0045	-.0245	.0172	-.0002
				11.9	.4065	.0055	-.0222	.0169	-.0007

TABLE III.- STATIC STABILITY AND CONTROL CHARACTERISTICS OF GLIDER -
Continued

M	Re, millions	δ_a, deg	δ_r, deg	α, deg	C_N	C_m	C_Y	C_n	C_l
1.1	2.5	0	0	-1.0	-0.0247	0.0094	0.0039	-0.0010	-0.0007
				0	0	.0077	.0037	-.0004	-.0006
				1.1	.0235	.0071	.0040	-.0002	-.0006
				2.2	.0533	.0068	.0043	.0002	-.0007
				3.3	.0868	.0055	.0045	.0004	-.0011
				5.5	.1643	.0030	.0059	.0010	-.0015
				7.9	.2483	-.0001	.0055	.0033	-.0013
				9.9	.3248	-.0008	.0079	.0029	-.0026
		-20	0	-1.0	-.0495	.0229	.0234	-.0236	-.0092
				0	-.0265	.0219	.0236	-.0232	-.0094
				1.1	-.0031	.0213	.0237	-.0225	-.0093
				2.2	.0258	.0206	.0238	-.0218	-.0092
				3.2	.0600	.0185	.0236	-.0206	-.0090
				5.4	.1382	.0142	.0220	-.0166	-.0080
				7.6	.2168	.0129	.0229	-.0151	-.0085
				9.8	.2934	.0144	.0260	-.0161	-.0102
		20	0	-1.0	-.0039	-.0022	-.0157	.0123	.0077
				0	.0193	-.0034	-.0163	.0132	.0079
				1.1	.0435	-.0038	-.0160	.0132	.0079
				2.2	.0731	-.0049	-.0158	.0133	.0078
				3.3	.1054	-.0054	-.0156	.0135	.0077
				5.4	.1822	-.0095	-.0140	.0129	.0072
				7.7	.2631	-.0108	-.0145	.0146	.0072
				9.9	.3421	-.0112	-.0154	.0168	.0073
				11.0	.3780	-.0098	-.0154	.0175	.0072
		0	30	-1.0	-.0191	.0071	-.0276	.0140	.0023
				0	.0046	.0059	-.0278	.0150	.0025
				1.1	.0272	.0054	-.0278	.0154	.0026
				2.2	.0555	.0051	-.0277	.0158	.0023
				3.3	.0880	.0044	-.0277	.0164	.0020
				5.4	.1637	.0012	-.0264	.0169	.0017
				7.6	.2438	-.0009	-.0269	.0191	.0018
				9.9	.3237	-.0007	-.0248	.0188	.0007
				11.0	.3634	-.0007	-.0244	.0190	.0003

TABLE III.- STATIC STABILITY AND CONTROL CHARACTERISTICS OF GLIDER -
Continued

M	Re, millions	δ_a, deg	δ_r, deg	α, deg	c_N	c_m	c_Y	c_n	c_l
1.3	2.5	0	0	-1.0	-0.0236	0.0103	0.0030	-0.0008	-0.0008
				.1	-.0001	.0085	.0030	-.0004	-.0008
				1.1	.0240	.0082	.0036	-.0002	-.0009
				2.3	.0542	.0070	.0037	.0003	-.0009
				3.4	.0894	.0052	.0043	.0006	-.0012
				5.7	.1635	.0020	.0053	.0010	-.0018
				7.9	.2408	-.0002	.0062	.0021	-.0021
				9.9	.3111	-.0012	.0069	.0031	-.0027
		-20	0	-1.0	-.0456	.0228	.0205	-.0214	-.0078
				0	-.0224	.0209	.0212	-.0214	-.0080
				1.1	.0011	.0204	.0216	-.0211	-.0080
				2.2	.0290	.0201	.0218	-.0205	-.0082
				3.3	.0625	.0178	.0220	-.0197	-.0081
				5.4	.1372	.0137	.0205	-.0158	-.0073
				7.7	.2125	.0113	.0213	-.0146	-.0079
				9.9	.2870	.0107	.0229	-.0144	-.0090
		20	0	-1.0	-.0034	-.0011	-.0150	.0119	.0076
				0	.0189	-.0021	-.0150	.0121	.0077
				1.1	.0441	-.0033	-.0149	.0123	.0076
				2.2	.0734	-.0042	-.0144	.0123	.0075
				3.3	.1047	-.0048	-.0140	.0122	.0072
				5.5	.1770	-.0085	-.0127	.0121	.0064
				7.7	.2490	-.0091	-.0134	.0140	.0067
				9.9	.3257	-.0105	-.0131	.0152	.0062
				11.0	.3631	-.0108	-.0132	.0157	.0062
		0	30	-1.0	-.0196	.0085	-.0210	.0104	.0016
				0	.0028	.0073	-.0210	.0108	.0016
				1.1	.0275	.0064	-.0208	.0111	.0016
				2.2	.0549	.0063	-.0205	.0115	.0014
				3.3	.0884	.0044	-.0205	.0120	.0012
				5.5	.1577	.0020	-.0225	.0146	.0010
				7.7	.2342	-.0008	-.0211	.0153	.0008
				9.9	.3086	-.0014	-.0205	.0160	.0001
				11.0	.3483	-.0034	-.0192	.0160	-.0003

TABLE III.- STATIC STABILITY AND CONTROL CHARACTERISTICS OF GLIDER -
Continued

M	Re, millions	δ_a, deg	δ_r, deg	α, deg	C_N	C_m	C_Y	C_n	C_l
3.0	5.3	0	0	3.6	0.0832	0.0011	0.0038	-0.0006	-0.0015
				-1.0	-.0050	.0051	.0027	-.0011	-.0010
				.1	.0146	.0044	.0030	-.0009	-.0010
				1.3	.0363	.0035	.0034	-.0009	-.0012
				2.4	.0583	.0027	.0037	-.0008	-.0014
				3.5	.0819	.0011	.0038	-.0007	-.0015
				4.7	.1050	0	.0039	-.0004	-.0017
				5.8	.1277	-.0009	.0042	-.0003	-.0018
				8.1	.1718	-.0025	.0044	-.0002	-.0020
		-20	0	3.6	.0608	.0057	.0092	-.0076	-.0035
				-1.0	-.0127	.0094	.0092	-.0094	-.0035
				.1	.0054	.0066	.0095	-.0093	-.0035
				1.3	.0218	.0079	.0095	-.0089	-.0036
				2.4	.0407	.0067	.0094	-.0083	-.0036
				3.5	.0602	.0057	.0093	-.0076	-.0035
				5.8	.0995	.0032	.0091	-.0063	-.0034
				8.1	.1366	.0014	.0091	-.0053	-.0034
				3.5	.0605	.0054	.0092	-.0075	-.0034
		20	0	3.6	.0950	-.0056	-.0050	.0042	.0033
				-1.0	.0062	-.0012	-.0056	.0042	.0035
				.2	.0264	-.0021	-.0060	.0049	.0035
				1.3	.0475	-.0031	-.0057	.0048	.0034
				2.4	.0707	-.0042	-.0055	.0048	.0032
				3.6	.0944	-.0057	-.0054	.0050	.0032
				5.9	.1408	-.0080	-.0049	.0050	.0030
				8.1	.1843	-.0092	-.0048	.0055	.0030
				3.6	.0943	-.0057	-.0053	.0048	.0033
		0	30	3.6	.0118	.0006	-.0100	.0072	.0016
				-1.0	-.0008	.0048	-.0100	.0058	.0018
				.1	.0020	.0040	-.0099	.0061	.0016
				1.3	.0050	.0032	-.0098	.0063	.0015
				2.4	.0083	.0022	-.0098	.0067	.0013
				3.5	.0117	.0005	-.0099	.0071	.0015
				5.8	.0183	-.0018	-.0099	.0078	.0013
				8.1	.0245	-.0033	-.0103	.0088	.0011
				3.5	.0118	.0005	-.0099	.0071	.0016

TABLE III.- STATIC STABILITY AND CONTROL CHARACTERISTICS OF GLIDER - Continued

M	Re, millions	δ_a, deg	δ_r, deg	α, deg	c_N	c_m	c_Y	c_n	c_l
4.0	5.2	0	0	3.3	0.0656	0.0011	0.0034	-0.0009	-0.0012
				-1.0	-.0066	.0053	.0024	-.0011	-.0007
				.1	.0106	.0044	.0028	-.0011	-.0007
				1.2	.0290	.0031	.0030	-.0010	-.0010
				2.2	.0476	.0019	.0033	-.0010	-.0011
				3.3	.0662	.0009	.0033	-.0008	-.0013
				4.4	.0847	-.0001	.0035	-.0006	-.0015
				5.5	.1028	-.0006	.0036	-.0005	-.0016
				7.6	.1391	-.0025	.0040	-.0002	-.0018
		-20	0	3.3	.0577	.0035	.0106	-.0091	-.0038
				-1.0	-.0162	.0113	.0106	-.0110	-.0040
				.1	.0009	.0101	.0108	-.0108	-.0040
				1.1	.0191	.0088	.0108	-.0104	-.0041
				2.2	.0381	.0074	.0108	-.0098	-.0041
				3.3	.0577	.0058	.0106	-.0092	-.0039
				5.5	.0954	.0035	.0105	-.0080	-.0040
				7.6	.1319	.0018	.0105	-.0070	-.0040
				3.3	.0577	.0060	.0105	-.0091	-.0038
		20	0	3.3	.0794	-.0061	-.0059	.0046	.0037
				-1.0	.0053	-.0009	-.0049	.0031	.0034
				.1	.0220	-.0020	-.0054	.0036	.0036
				1.2	.0409	-.0031	-.0055	.0039	.0037
				2.2	.0602	-.0047	-.0057	.0043	.0037
				3.3	.0800	-.0063	-.0059	.0046	.0037
				5.5	.1173	-.0080	-.0064	.0052	.0037
				7.6	.1548	-.0106	-.0069	.0061	.0038
				3.3	.0795	-.0061	-.0063	.0053	.0037
		0	30	3.3	.0095	.0003	-.0105	.0069	.0020
				-1.0	-.0009	.0049	-.0097	.0056	.0021
				.1	.0015	.0040	-.0098	.0059	.0021
				1.1	.0041	.0028	-.0100	.0061	.0020
				2.2	.0068	.0015	-.0103	.0066	.0020
				3.3	.0094	.0004	-.0105	.0069	.0019
				5.5	.0148	-.0017	-.0112	.0079	.0018
				7.6	.0199	-.0037	-.0120	.0090	.0018
				3.3	.0094	.0003	-.0105	.0070	.0019

TABLE III.- STATIC STABILITY AND CONTROL CHARACTERISTICS OF GLIDER -
Continued

M	Re, millions	δ_a, deg	δ_r, deg	α, deg	c_N	c_m	c_Y	c_n	c_l
5.0	2.3	0	0	3.1	0.0554	0.0004	0.0031	-0.0009	0
				-1.0	-.0060	.0041	.0022	-.0009	.0002
				0	.0092	.0030	.0025	-.0009	0
				1.1	.0258	.0016	.0029	-.0010	-.0002
				2.1	.0416	.0006	.0031	-.0011	-.0003
				3.1	.0564	-.0001	.0037	-.0013	-.0004
				4.1	.0719	-.0009	.0039	-.0013	-.0005
				5.2	.0869	-.0017	.0042	-.0013	-.0008
				6.2	.1031	-.0025	.0044	-.0012	-.0009
				7.2	.1186	-.0033	.0044	-.0010	-.0011
		-20	0	3.1	.0439	.0070	.0105	-.0092	-.0033
				-1.0	-.0175	.0113	.0106	-.0108	-.0045
				0	.0060	.0065	.0107	-.0106	-.0033
				1.1	.0142	.0086	.0105	-.0100	-.0030
				2.1	.0305	.0071	.0107	-.0099	-.0030
				3.1	.0457	.0061	.0102	-.0089	-.0026
				5.2	.0770	.0039	.0103	-.0083	-.0025
				7.2	.1093	.0021	.0105	-.0075	-.0031
				3.1	.0469	.0055	.0104	-.0090	-.0020
		20	0	3.1	.0688	-.0063	-.0091	.0089	.0049
				-1.0	.0043	-.0011	-.0062	.0064	.0038
				0	.0209	-.0028	-.0071	.0073	.0040
				1.1	.0376	-.0044	-.0079	.0079	.0044
				2.1	.0546	-.0060	-.0085	.0085	.0048
				3.1	.0699	-.0071	-.0087	.0086	.0050
				5.2	.1022	-.0096	-.0099	.0097	.0053
				7.2	.1357	-.0121	-.0112	.0110	.0055
				3.1	.0702	-.0072	-.0085	.0085	.0049
		0	30	3.1	.0077	.0007	-.0114	.0072	.0030
				-1.0	-.0010	.0046	-.0098	.0053	.0031
				0	.0012	.0034	-.0102	.0059	.0034
				1.1	.0034	.0022	-.0106	.0063	.0036
				2.1	.0056	.0013	-.0112	.0069	.0035
				3.1	.0078	.0005	-.0119	.0080	.0032
				5.2	.0122	-.0013	-.0130	.0090	.0032
				7.2	.0167	-.0031	-.0138	.0099	.0031
				3.1	.0077	.0005	-.0118	.0079	.0032

TABLE III.- STATIC STABILITY AND CONTROL CHARACTERISTICS OF GLIDER -
Continued

M	Re, millions	δ_a, deg	δ_r, deg	α, deg	C_N	C_m	C_Y	C_n	C_l
6.0	1.3	0	0	3.1	0.0513	-0.0006	0.0053	-0.0025	0.0005
				-1.0	-.0005	.0011	.0049	-.0032	.0021
				0	.0112	.0010	.0051	-.0029	.0019
				1.0	.0245	.0004	.0053	-.0030	.0017
				2.0	.0384	-.0002	.0053	-.0028	.0015
				3.1	.0521	-.0010	.0055	-.0027	.0010
				4.1	.0655	-.0013	.0058	-.0026	.0007
				5.1	.0793	-.0018	.0059	-.0024	.0007
				6.1	.0931	-.0024	.0059	-.0020	.0004
				7.1	.1077	-.0031	.0060	-.0018	.0004
		-20	0	3.1	.0421	.0045	.0091	-.0073	-.0003
				-1.0	-.0105	.0069	.0097	-.0094	-.0004
				0	.0018	.0066	.0099	-.0093	.0006
				1.0	.0150	.0057	.0095	-.0083	-.0004
				2.0	.0270	.0059	.0092	-.0077	-.0004
				3.0	.0364	.0067	.0095	-.0078	-.0005
				5.1	.0697	.0029	.0094	-.0068	-.0007
				7.1	.0972	.0017	.0097	-.0063	-.0010
				3.1	.0426	.0041	.0093	-.0077	-.0006
		20	0	3.1	.0672	-.0075	-.0079	.0093	.0065
				-1.0	.0109	-.0033	-.0052	.0070	.0052
				0	.0247	-.0046	-.0061	.0079	.0055
				1.0	.0388	-.0055	-.0065	.0082	.0060
				2.0	.0533	-.0066	-.0072	.0089	.0063
				3.1	.0674	-.0075	-.0077	.0092	.0068
				5.1	.0965	-.0095	-.0095	.0109	.0071
				6.1	.1120	-.0111	-.0105	.0118	.0076
				7.1	.1274	-.0121	-.0112	.0125	.0081
				3.1	.0677	-.0078	-.0080	.0094	.0069
		0	30	3.1	.0074	-.0013	-.0109	.0073	.0055
				-1.0	0	.0009	-.0082	.0050	.0053
				0	.0017	.0006	-.0086	.0053	.0049
				1.0	.0036	0	-.0090	.0058	.0051
				2.0	.0055	-.0006	-.0101	.0068	.0054
				3.1	.0074	-.0011	-.0106	.0071	.0055
				5.1	.0112	-.0024	-.0123	.0085	.0054
				6.6	.0142	-.0035	-.0132	.0093	.0059
				7.1	.0153	-.0040	-.0138	.0097	.0059
				3.1	.0075	-.0017	-.0111	.0076	.0055

TABLE III.- STATIC STABILITY AND CONTROL CHARACTERISTICS OF GLIDER –
Concluded

M	Re, millions	δ_a, deg	α, deg	C_N	C_m	C_Y	C_n	C_l
12.2	3.7	0	1.0	0.0111	0.0019	0.0013	0.0001	0.0003
			2.1	.0211	.0016	.0005	-.0002	.0003
			3.1	.0310	.0012	.0012	-.0008	.0003
			4.1	.0396	.0012	.0018	-.0012	.0001
			5.1	.0477	.0012	.0028	-.0019	0
			6.1	.0563	.0004	.0031	-.0018	.0001
			7.1	.0759	0	.0033	-.0020	.0003
		-20	1.0	.0030	.0082	.0088	-.0105	-.0033
			2.1	.0138	.0072	.0088	-.0102	-.0032
			3.1	.0238	.0069	.0086	-.0100	-.0030
			4.0	.0347	.0058	.0090	-.0101	-.0028
			5.1	.0447	.0054	.0092	-.0101	-.0028
			5.7	.0483	.0056	.0101	-.0110	-.0030
		20	1.0	.0183	-.0026	-.0061	.0047	.0031
			2.0	.0271	-.0035	-.0069	.0055	.0034
			3.1	.0378	-.0052	-.0079	.0068	.0041
			4.0	.0476	-.0067	-.0094	.0083	.0050
			6.1	.0708	-.0095	-.0114	.0103	.0062

DECLASSIFIED

NOTE: All linear dimensions
in inches
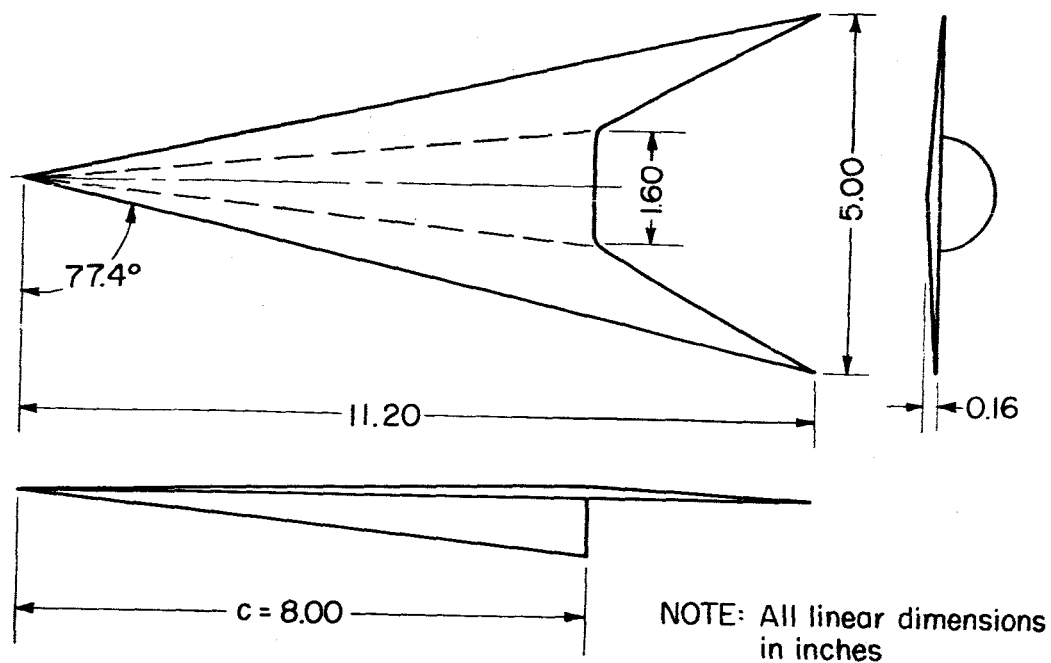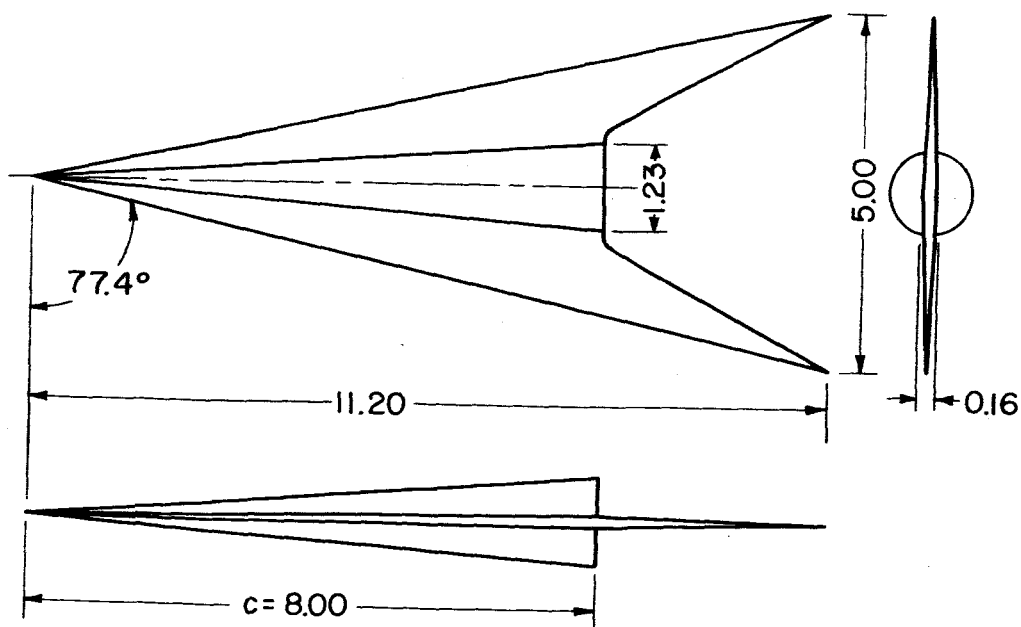
(a) Asymmetric model.

(b) Symmetric model.

Figure 1.- Scale models used to study effects of aerodynamic interference.

(a) Asymmetric model.

NOTE: All linear dimensions in inches.
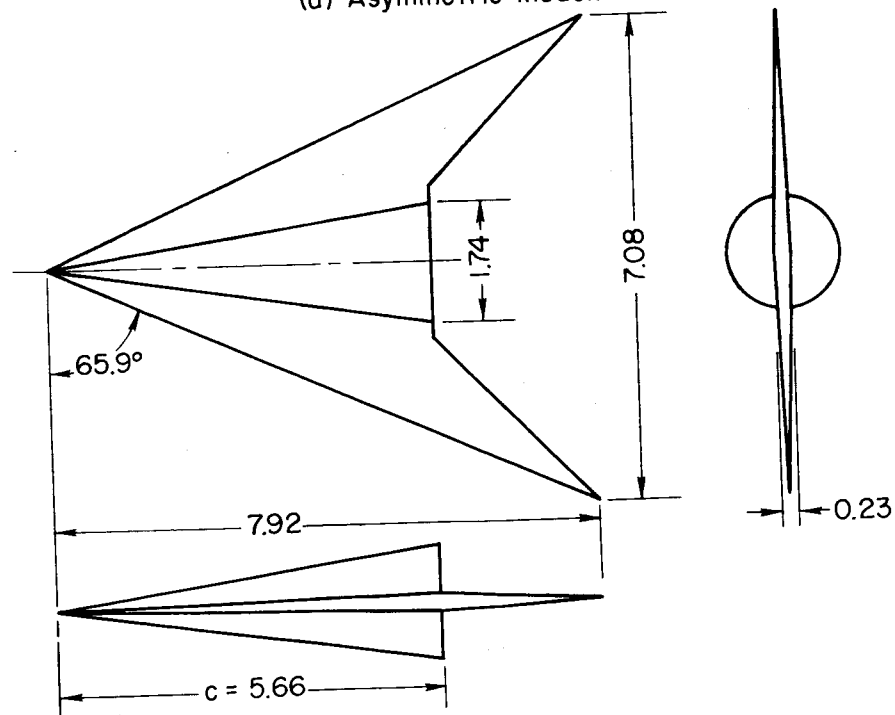
(b) Symmetric model.

Figure 2.- Hypersonically similar models used to study effects of aerodynamic interference.

X	Y
0	0
.1	.0258
.25	.0513
.50	.0863
.75	.1170
1.0	.1452
1.5	.1969
2.0	.2441
2.5	.2885
3.0	.3309
3.5	.3717
4.0	.4105
4.5	.4483
5.0	.4854
5.5	.5212
6.0	.5565
6.5	.5912
7.0	.6250

NOTE: All linear dimensions in inches
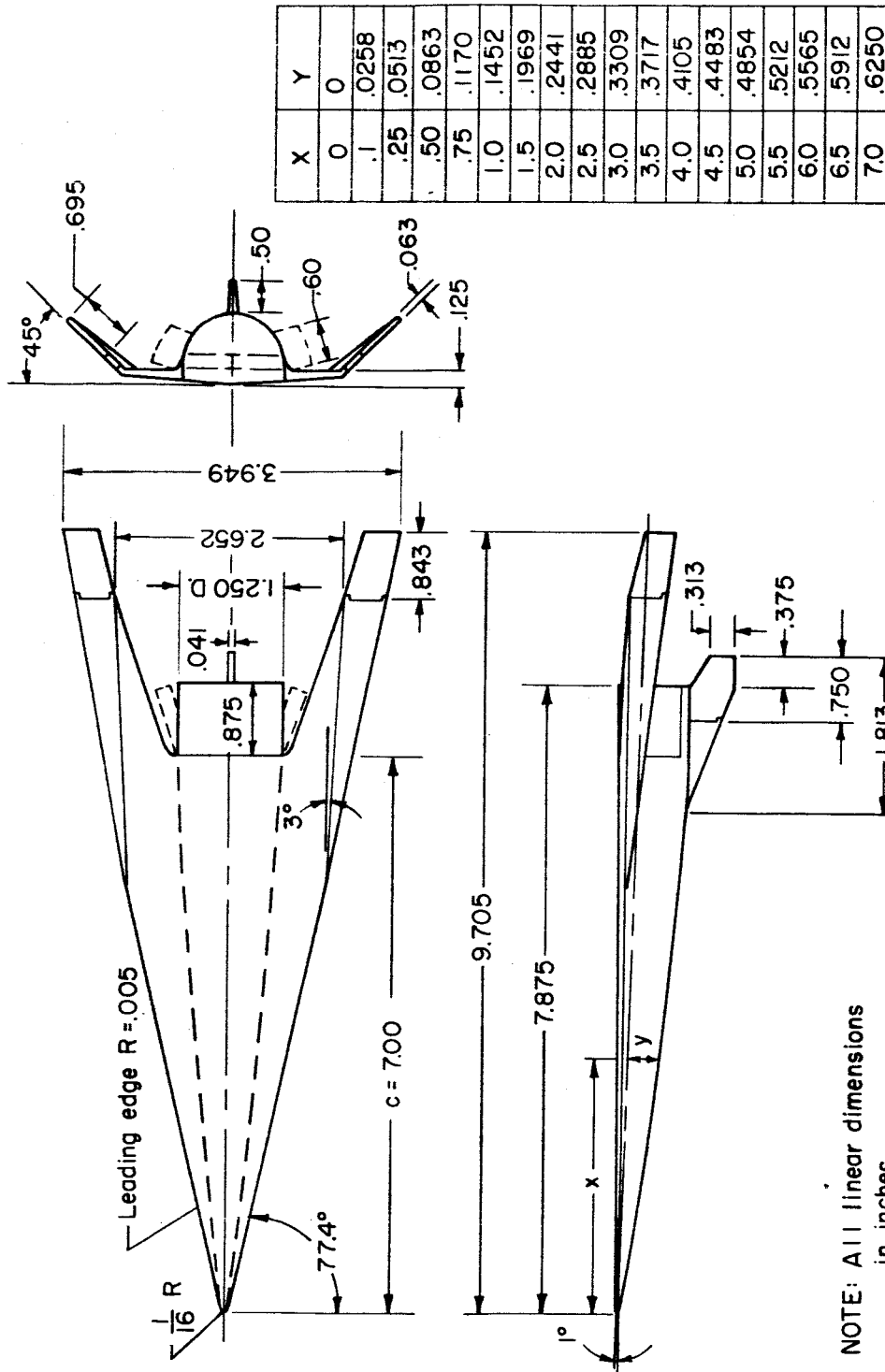
(a) Scale model.

Figure 3.- Glider models.

x inches	y inches
0	0
.010	.0084
.050	.0238
.100	.0474
.250	.0942
.500	.1584
.750	.2147
1.000	.2664
1.500	.3611
2.000	.4480
2.500	.5297
3.000	.6073
3.500	.6817
4.000	.7535
4.500	.8232
4.949	.8840

NOTE: All linear dimensions in inches

(b) Hypersonically similar model.

Figure 3.- Concluded.
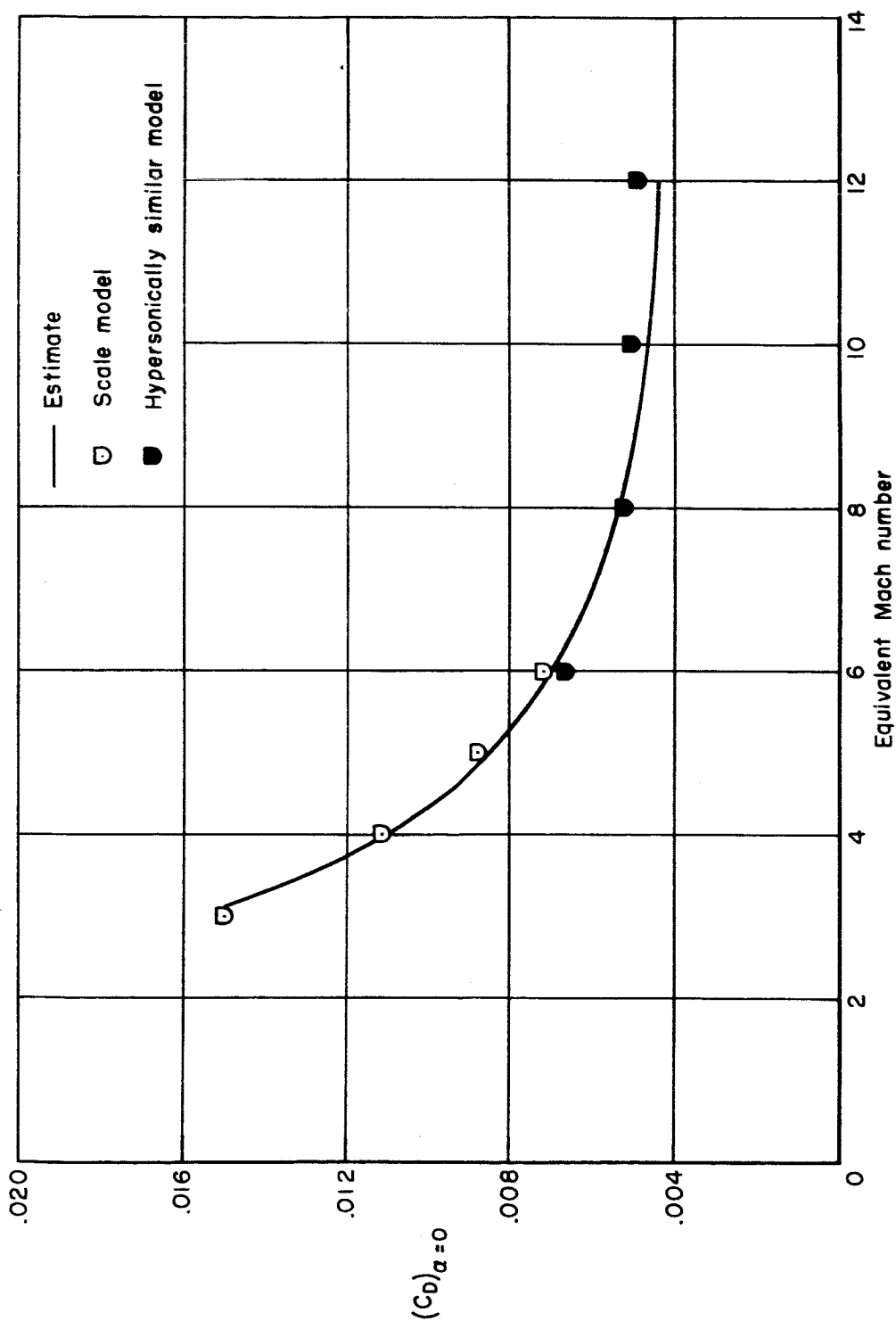
Figure 4.- Drag coefficient at $\alpha = 0^\circ$ for the asymmetric model (friction drag adjusted to assumed flight conditions).
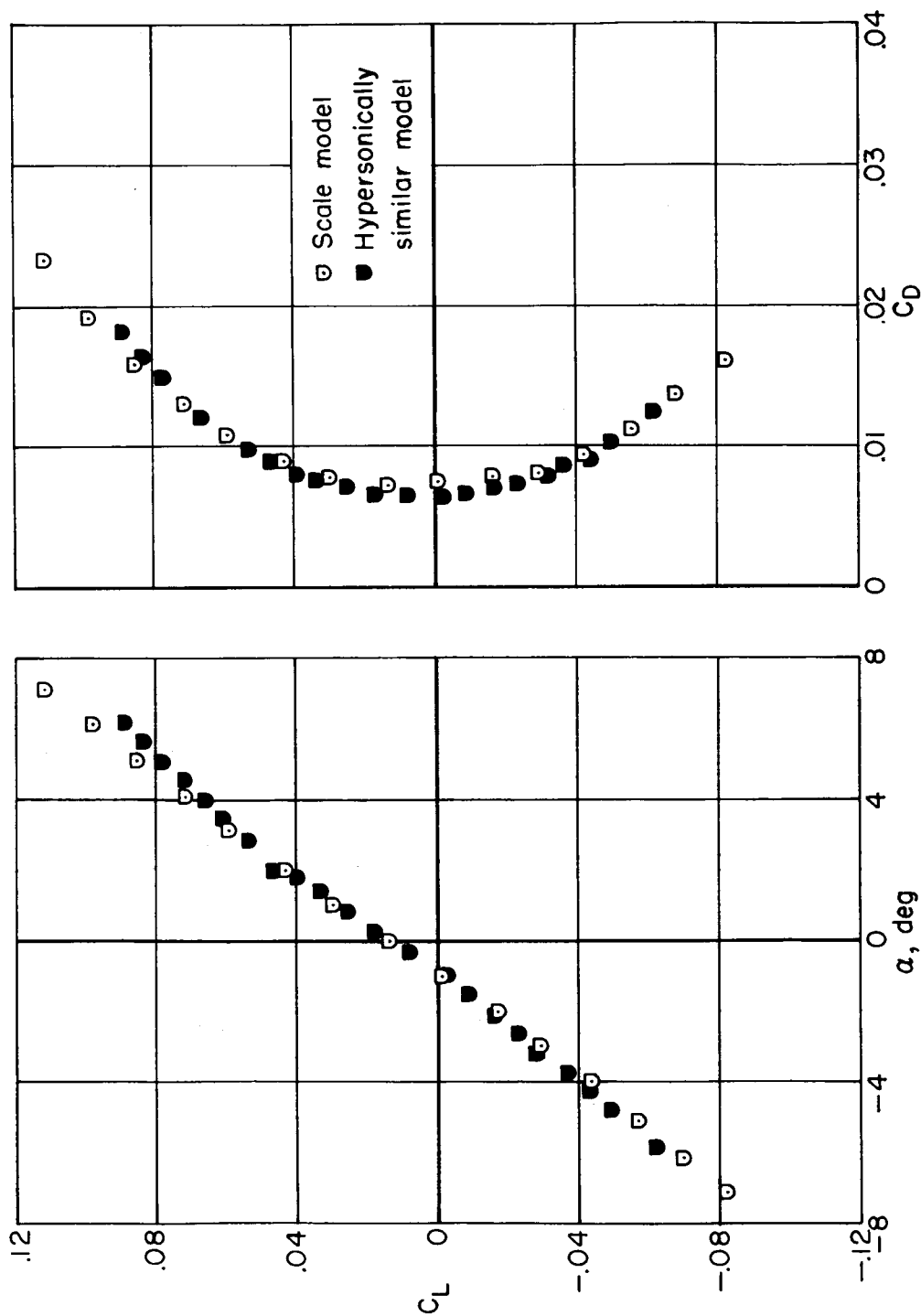
Figure 5.- Lift curve and drag polar for asymmetric model at an equivalent Mach number of 6.
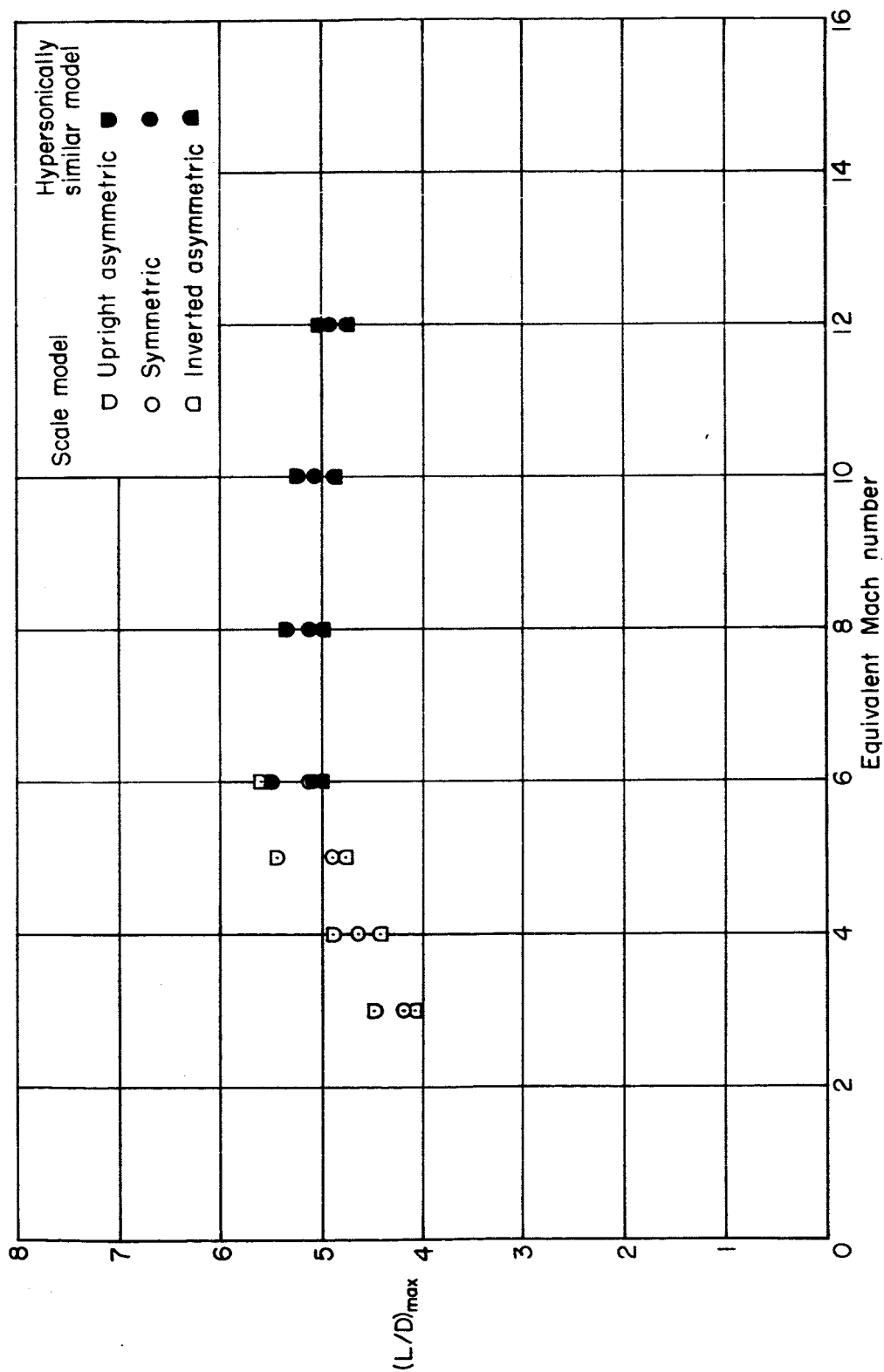
Figure 6.- Aerodynamic performance at Mach numbers from 3 to 12.
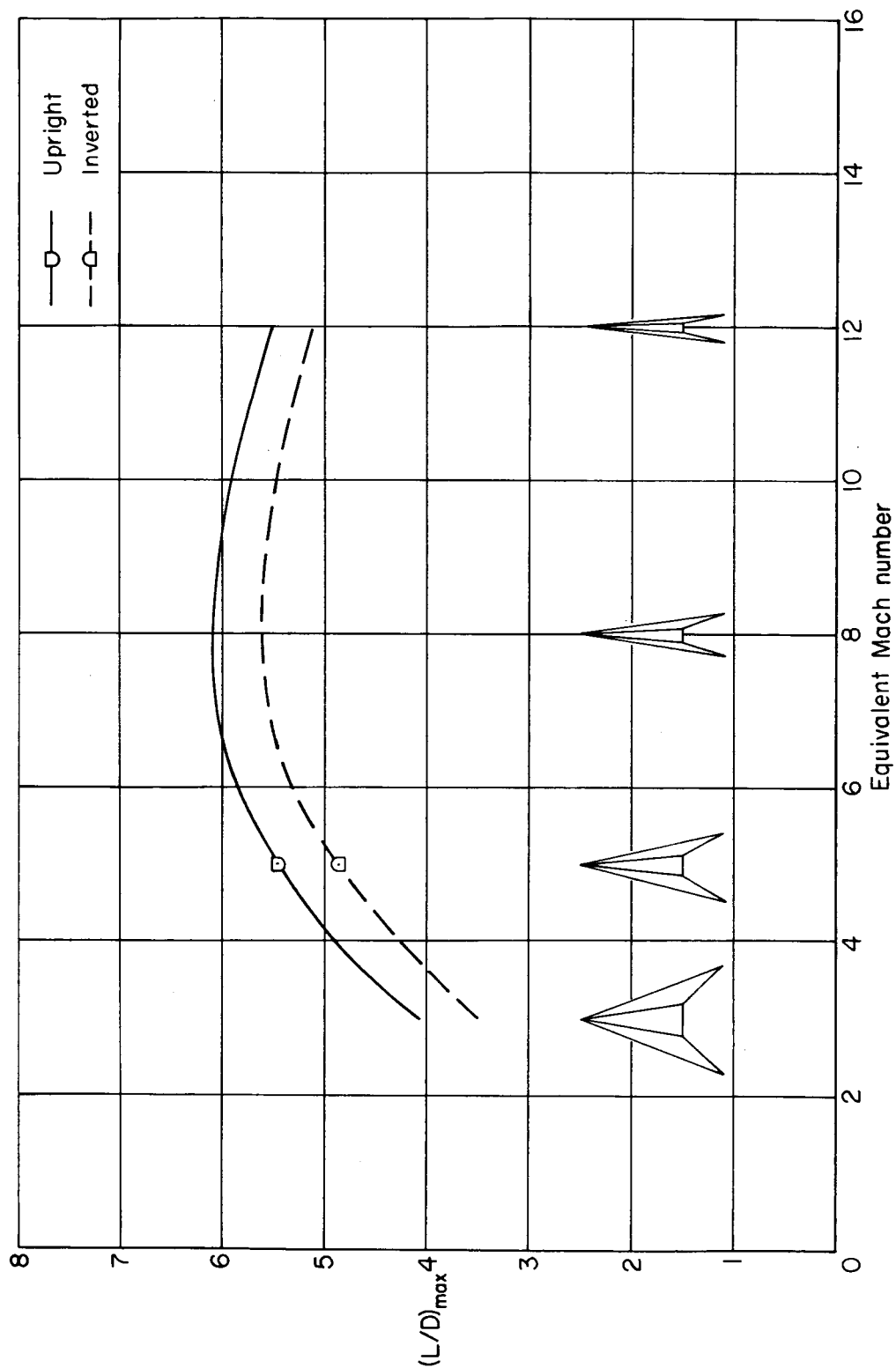
Figure 7.- Aerodynamic performance of asymmetric configurations at design Mach number.

32.50'

10.25'

Leading edge dia. = 3/8"

4" dia. nose

77.4°

58.0'

80.5'

65.2'

1°
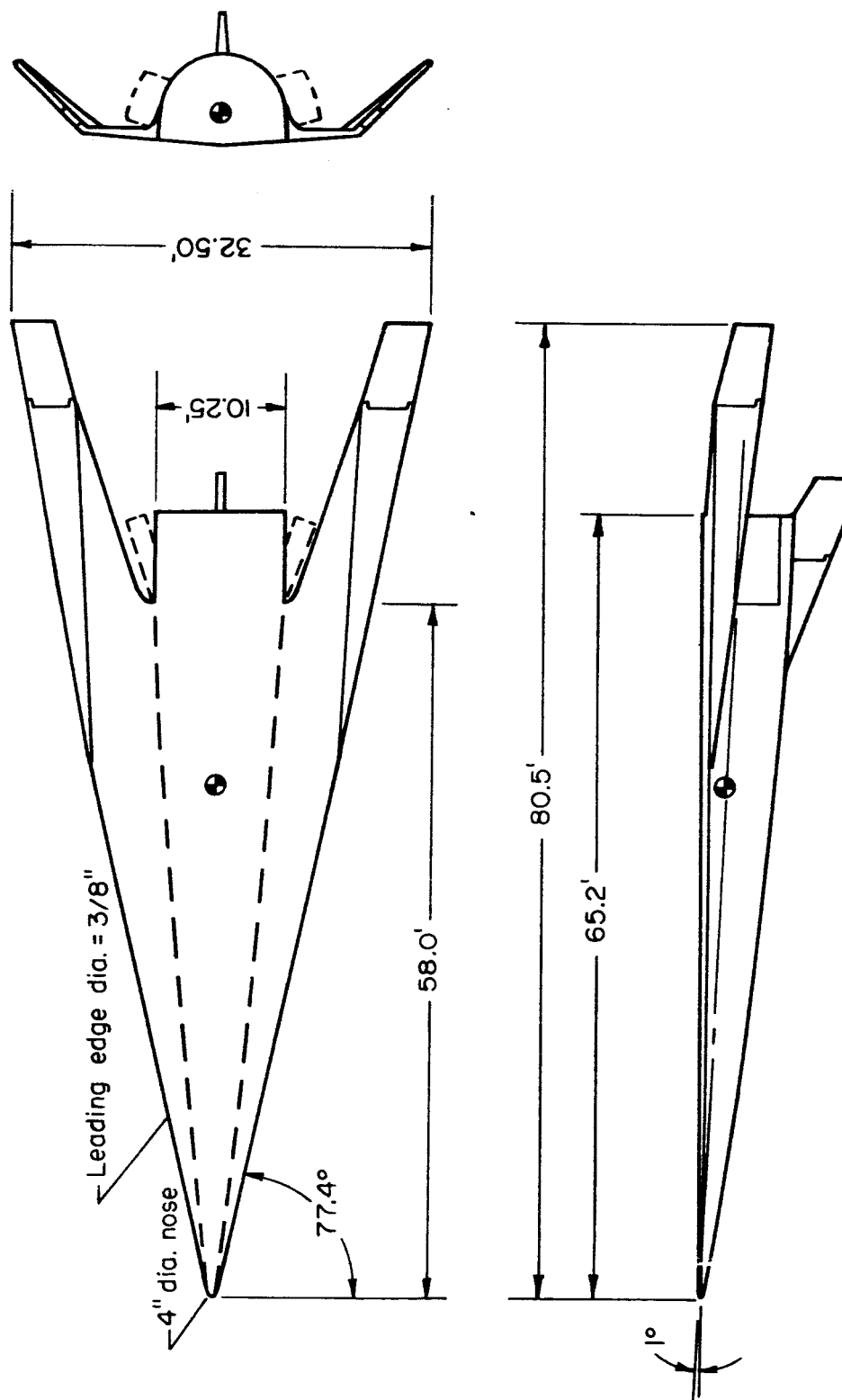
Figure 8.- Glider configuration.
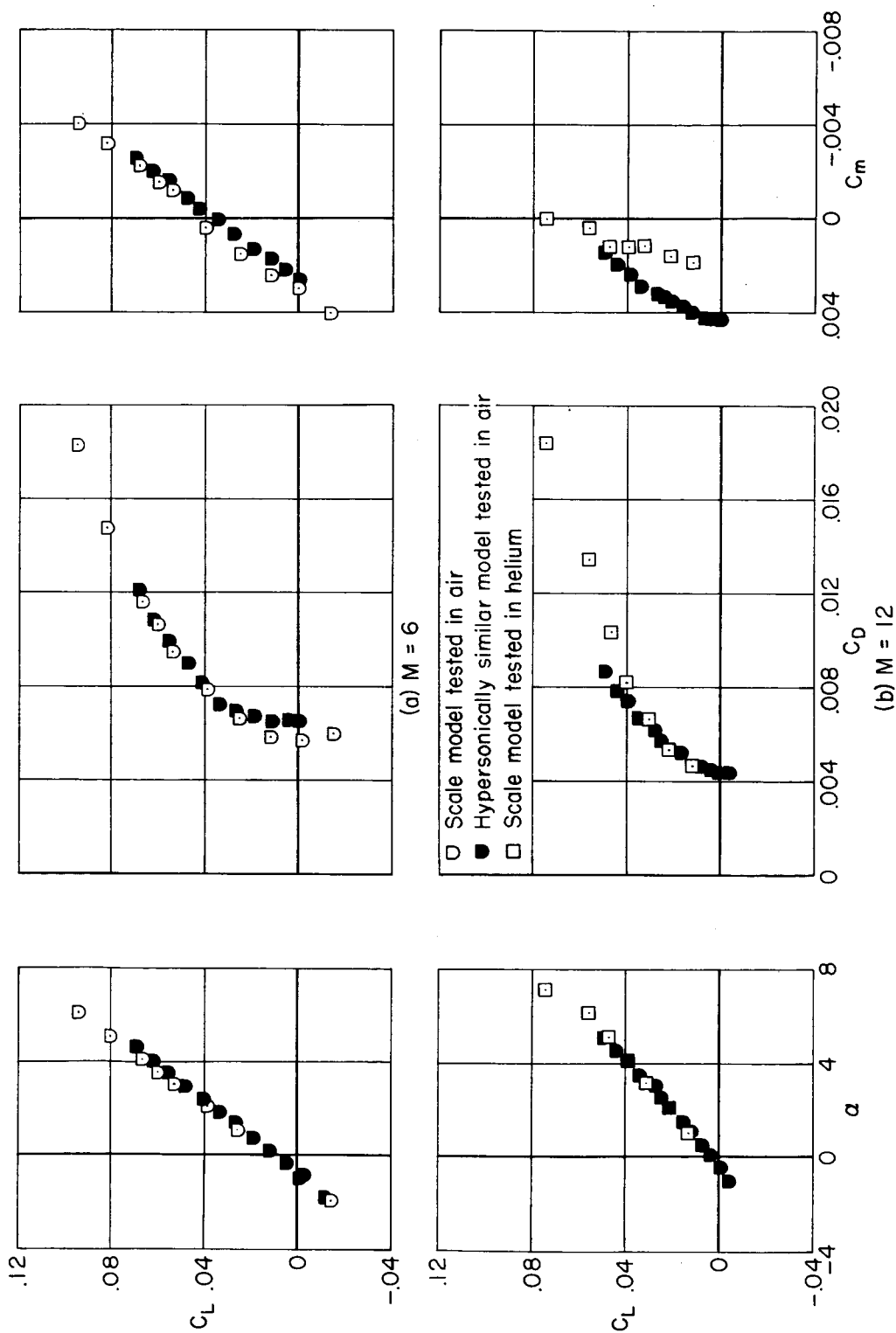
Figure 9.- Aerodynamic characteristics of glider.
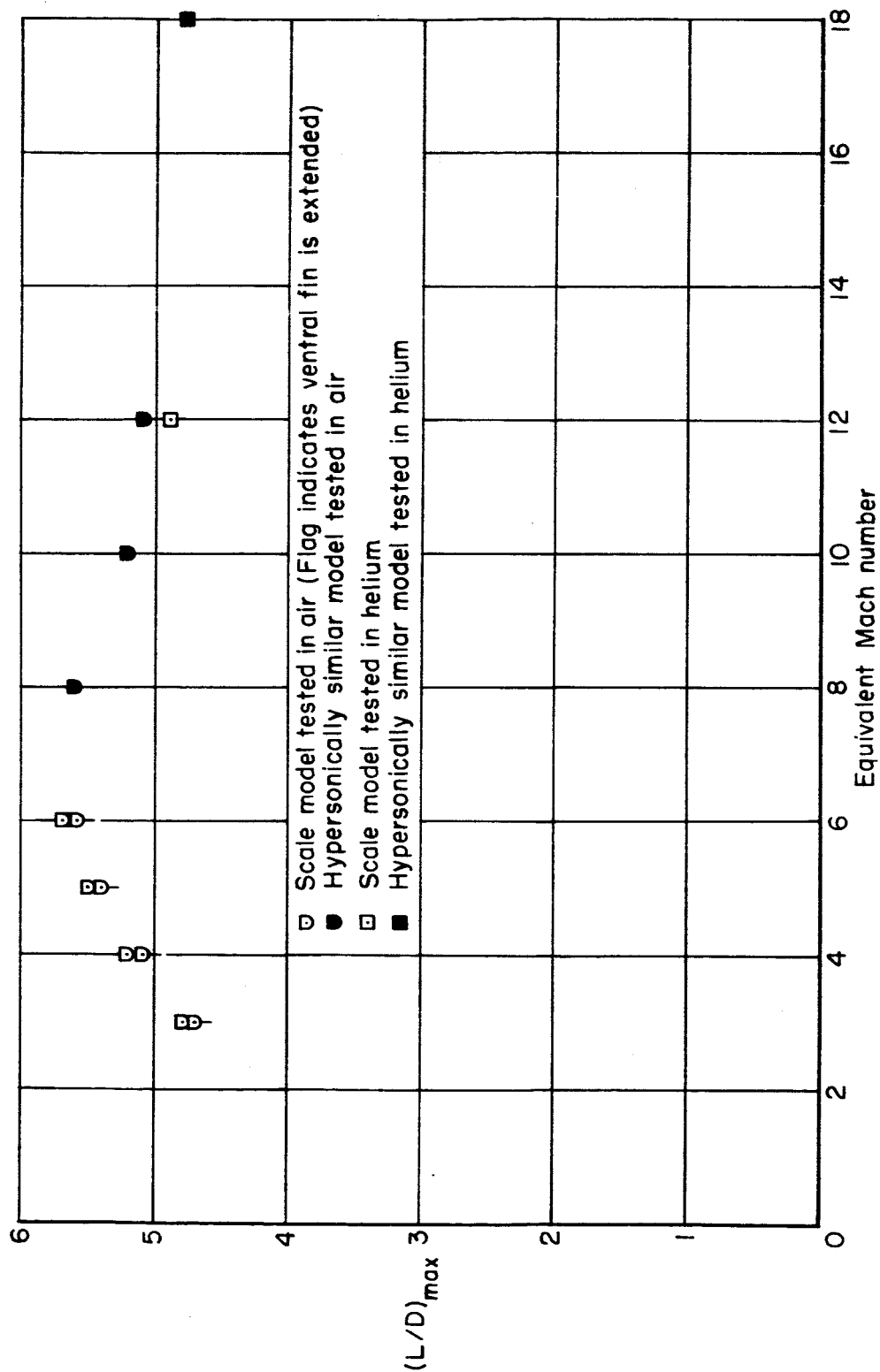
Figure 10.- Aerodynamic performance of glider at Mach numbers from 3 to 18.
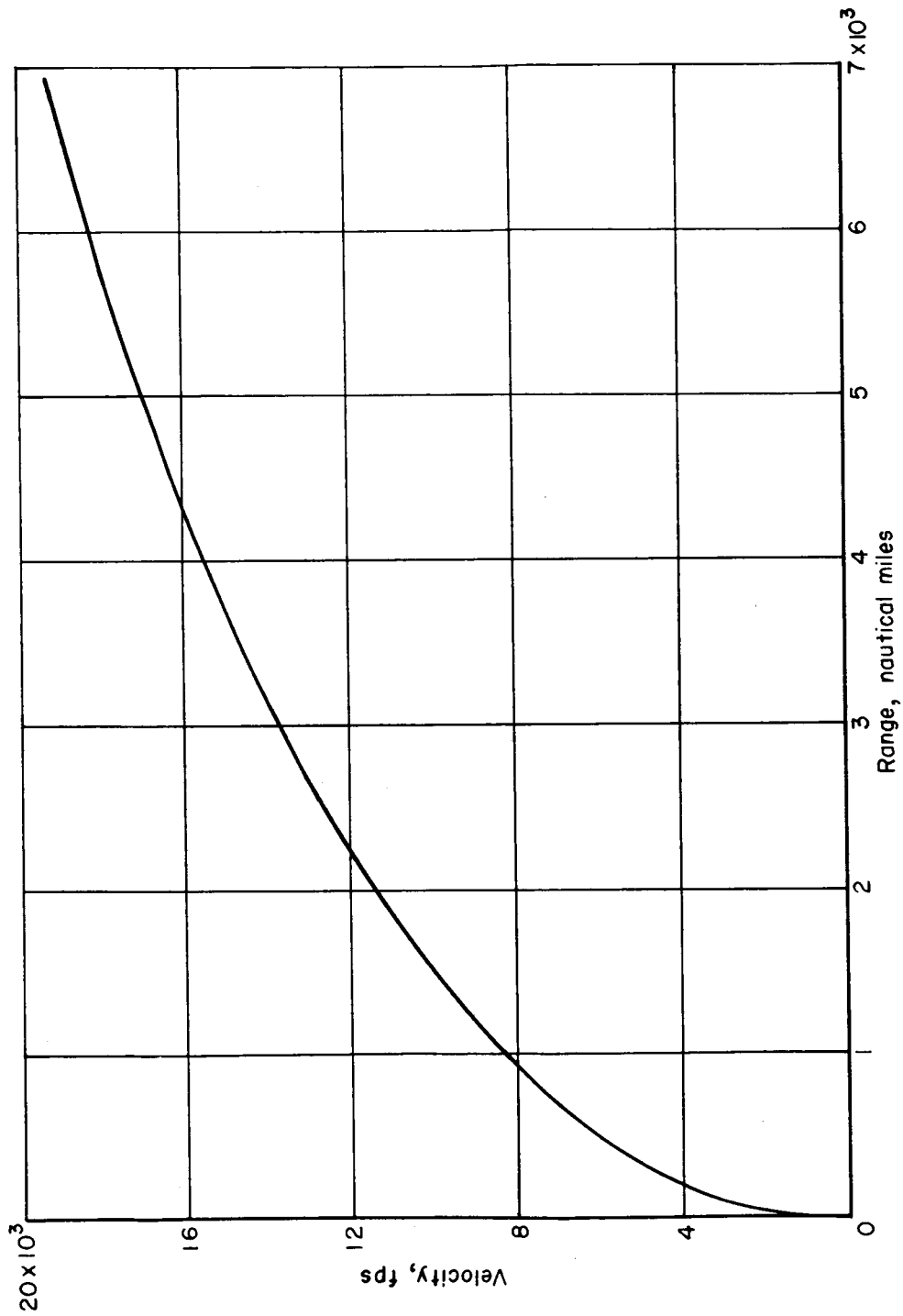
Figure 11.- Estimated range capabilities of glider.

(a) M = 0.6

(b) M = 1.3
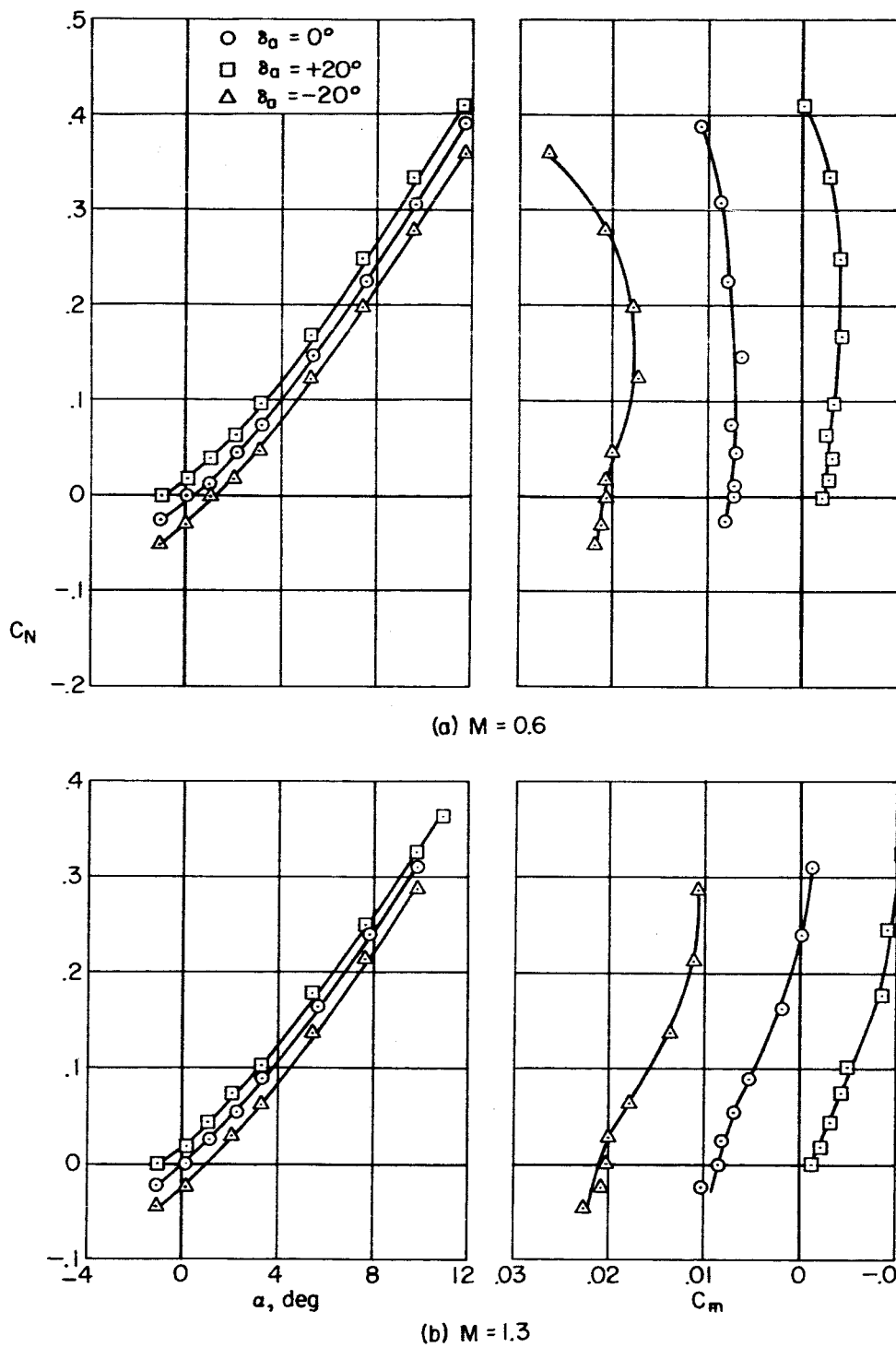
Figure 12.- Static longitudinal stability and control characteristics of glider.
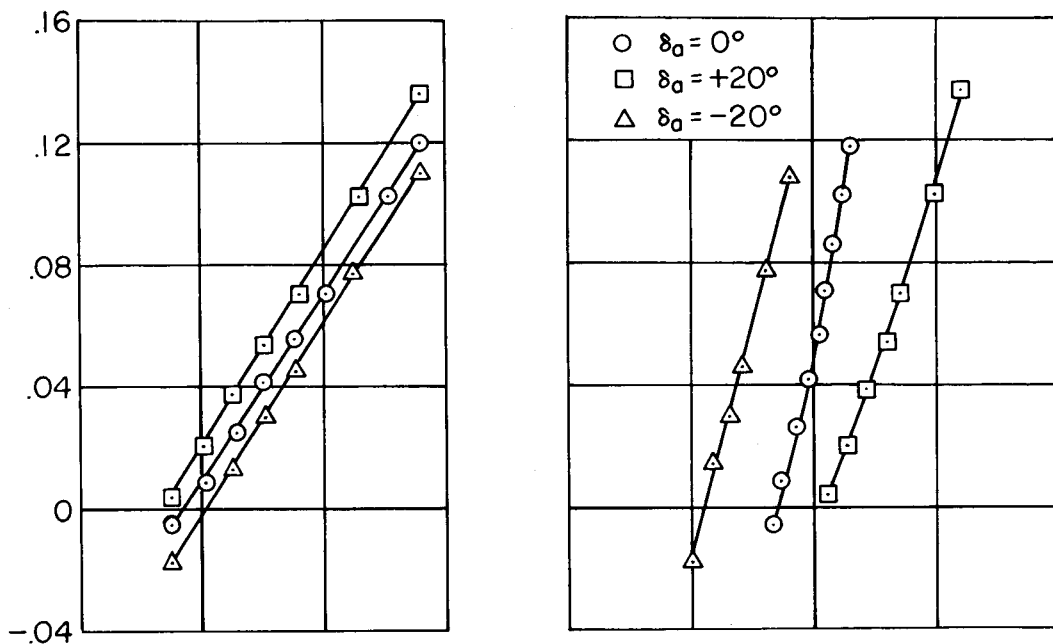
(c) M = 5
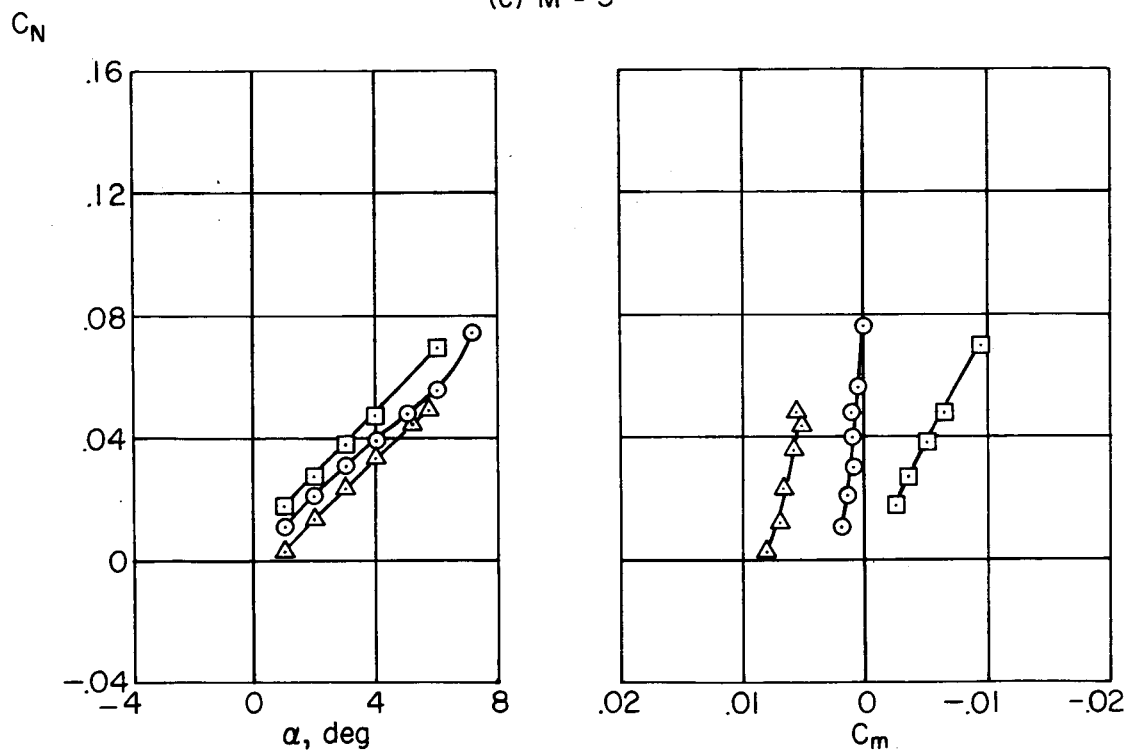
(d) M = 12

Figure 12.- Concluded.
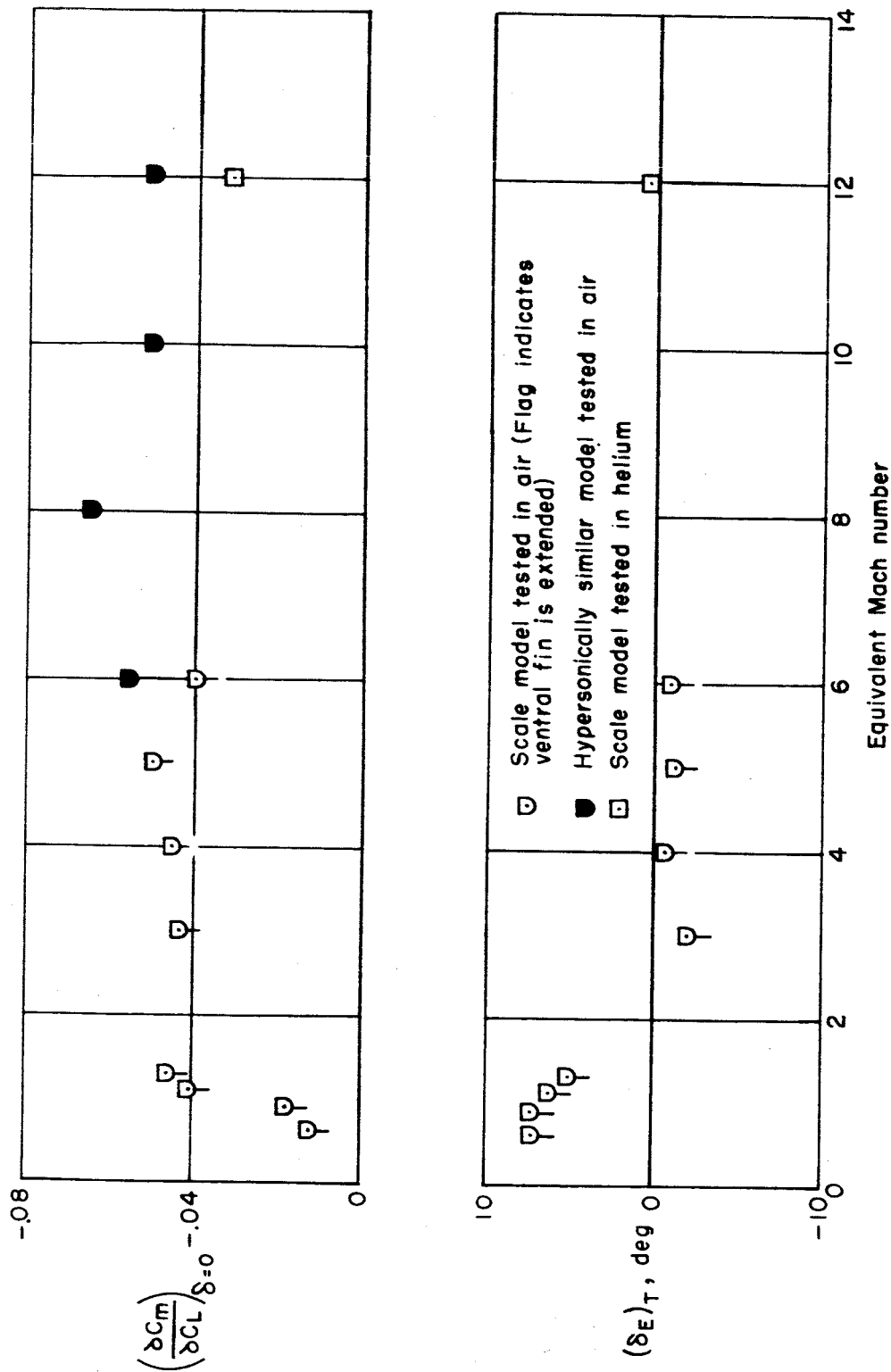
Figure 13.- Longitudinal stability and control at $\alpha = 5°$.
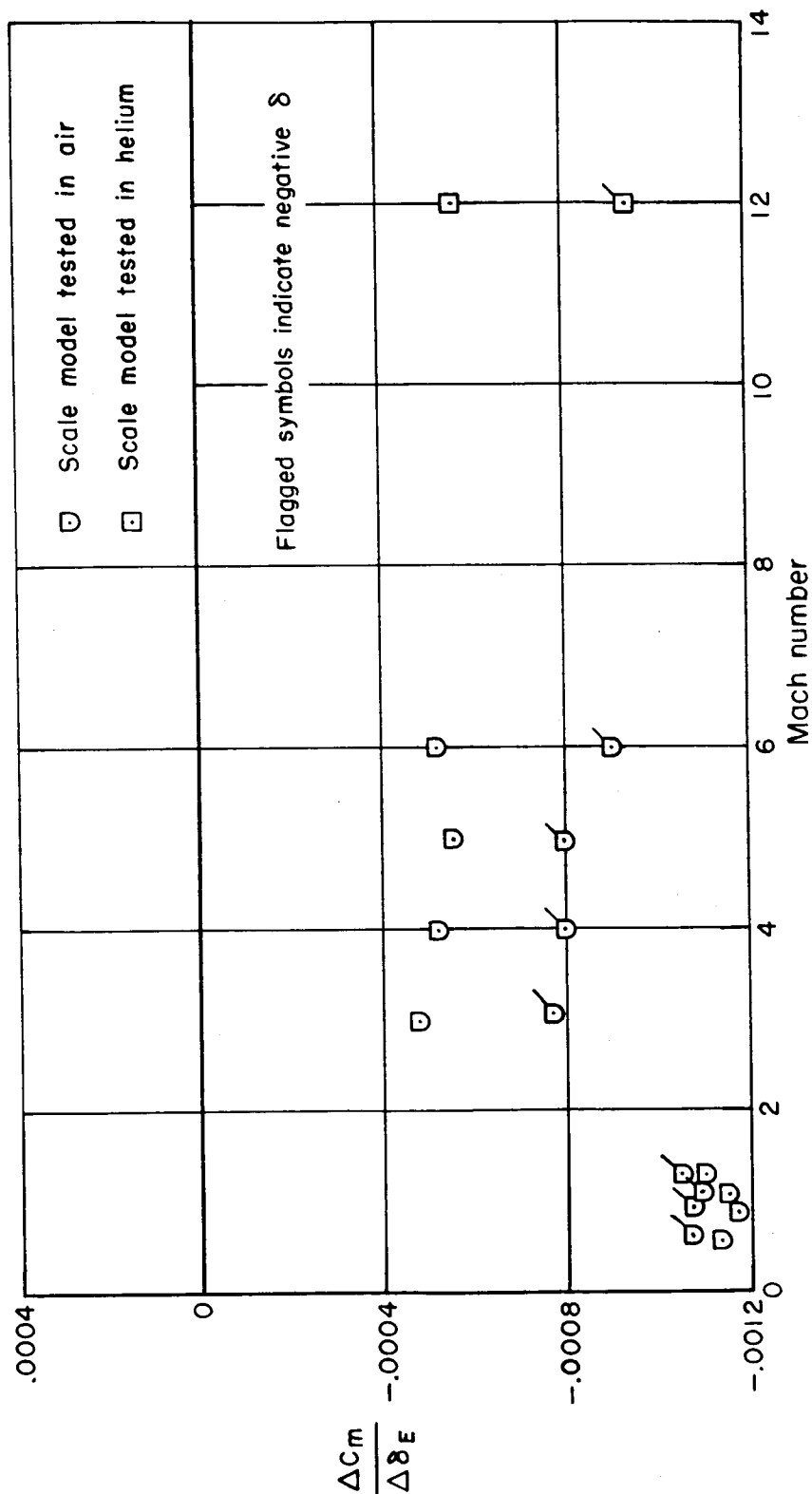
Figure 14.- Elevator effectiveness at $\alpha = 5^{\circ}$.

(a) $\alpha = 0°$

(b) $\alpha = 3°$

(c) $\alpha = 7°$
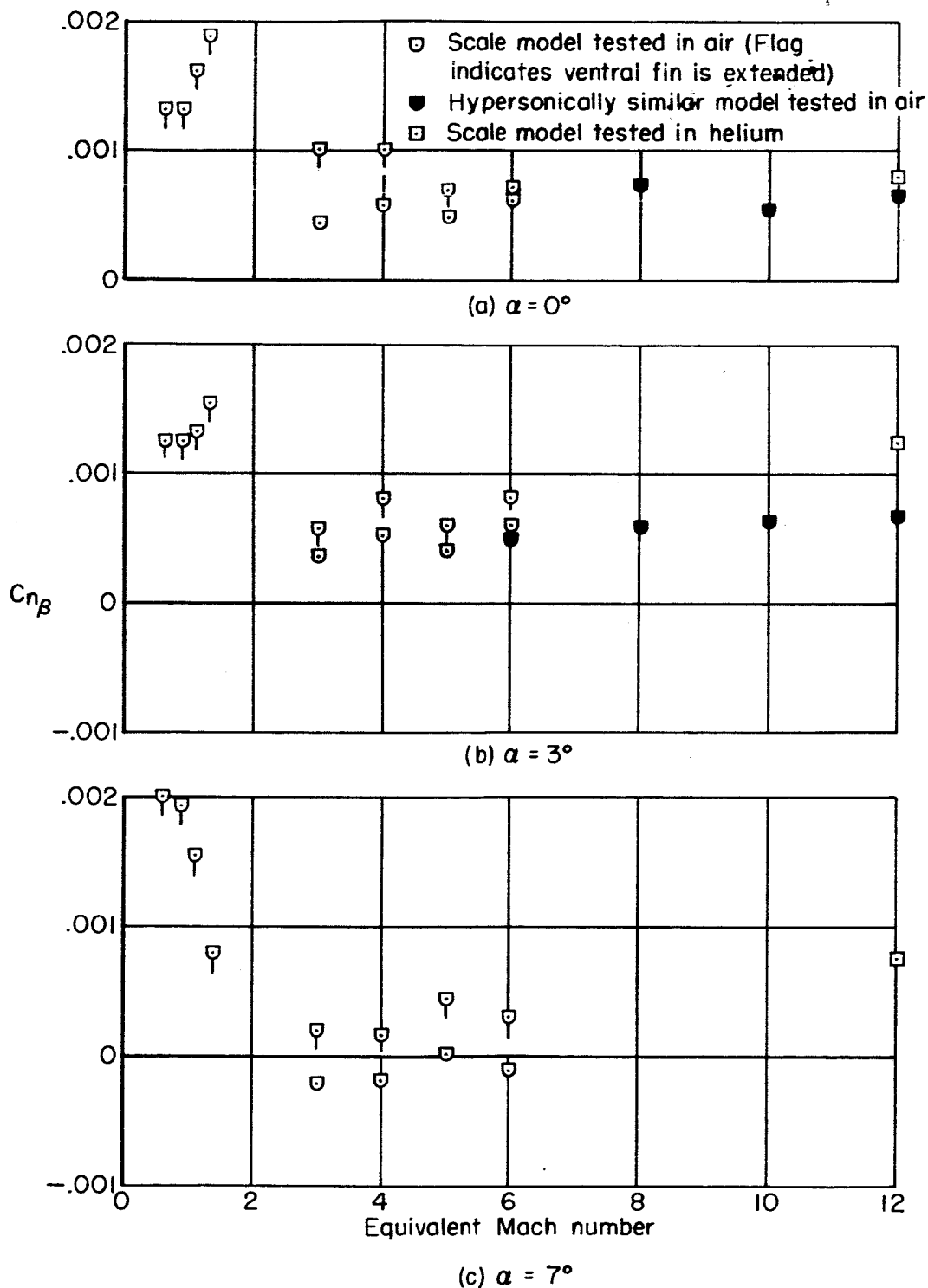
Figure 15.- Directional-stability characteristics of glider.
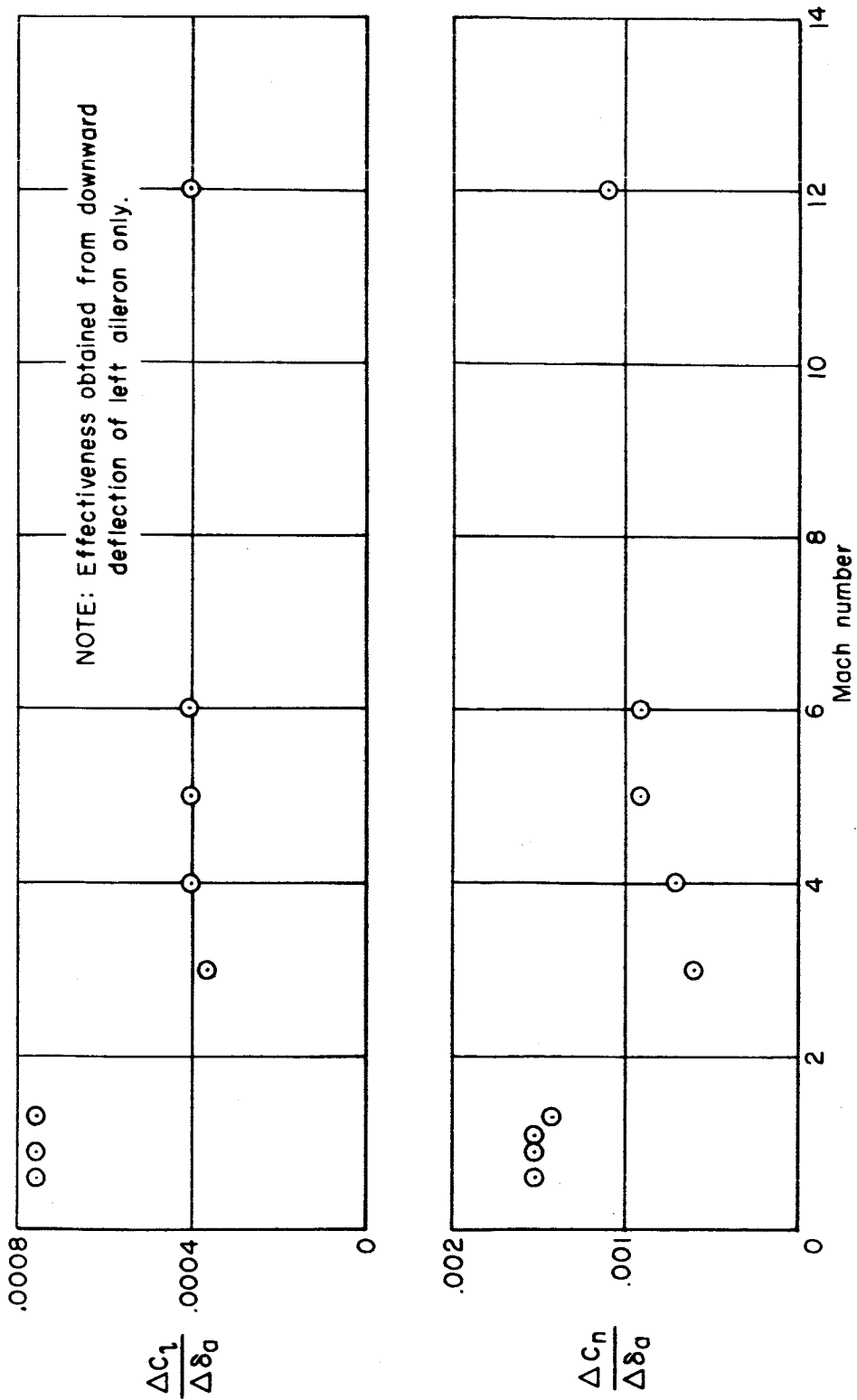
(a) $\alpha = 0°$

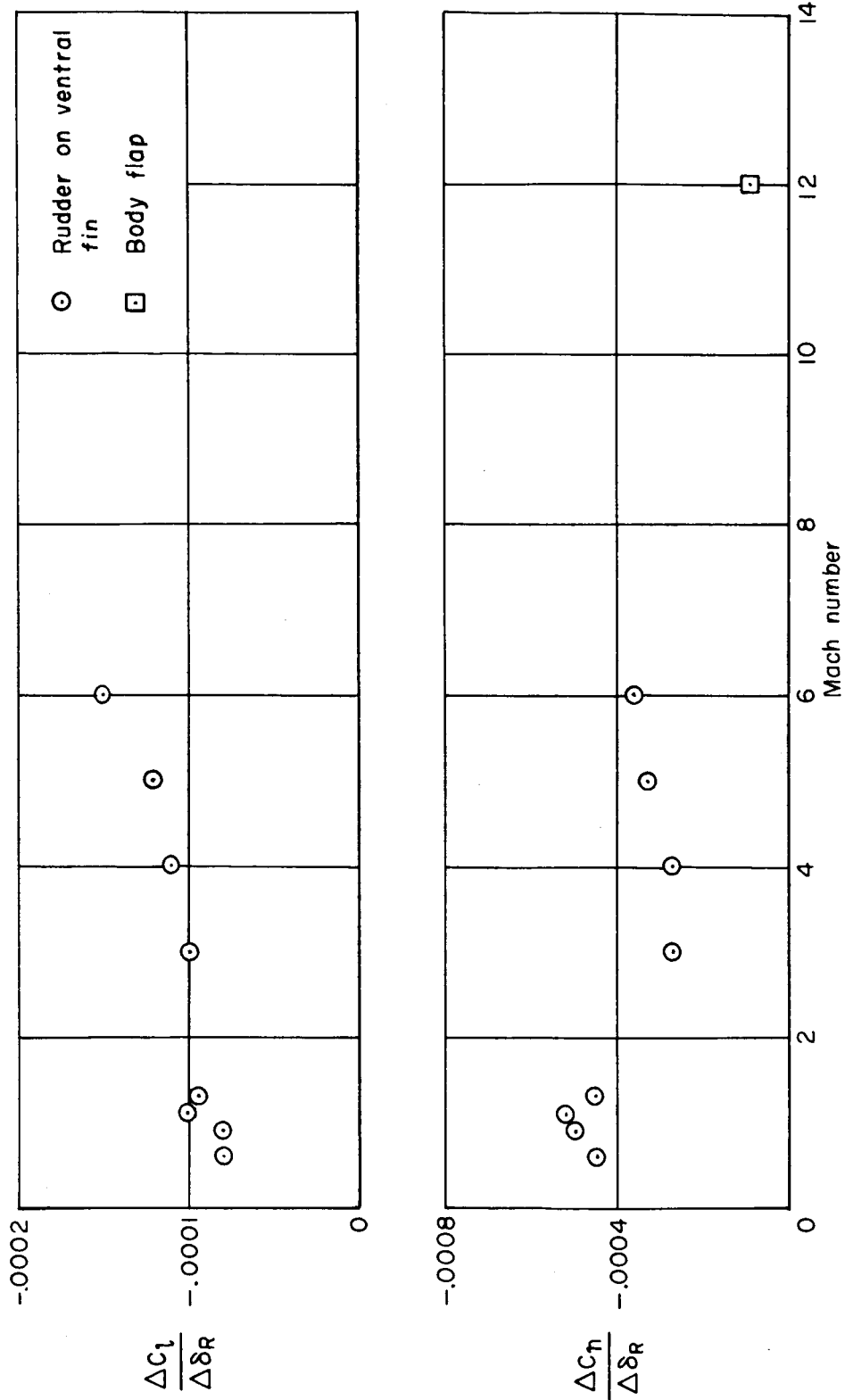(b) $\alpha = 3°$

(c) $\alpha = 7°$
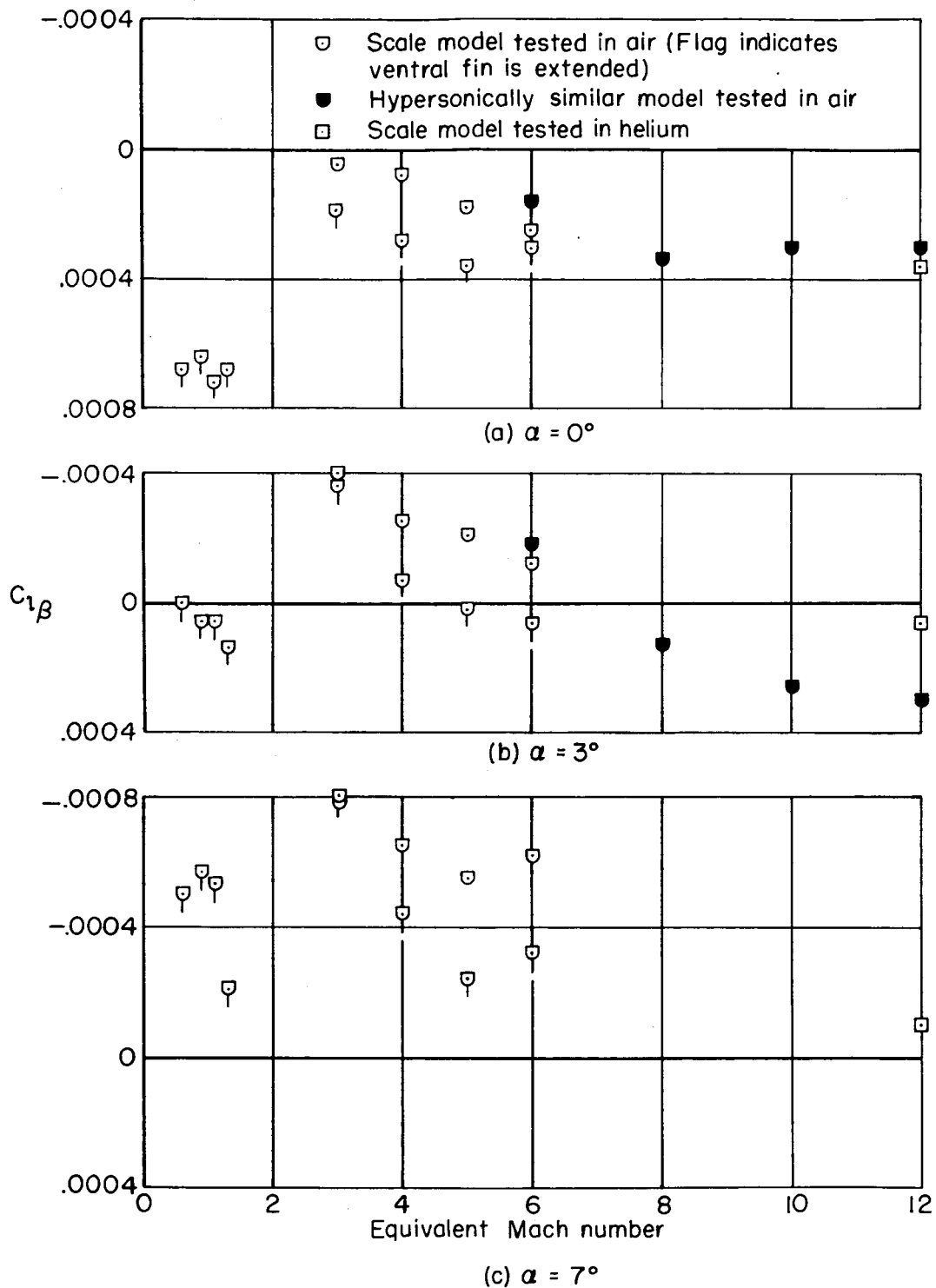
Figure 16.- Lateral-stability characteristics of glider.

(a) Aileron effectiveness.

Figure 17.- Directional and lateral control characteristics at $\alpha = 5^{\circ}$.

(b) Rudder effectiveness.

Figure 17.- Concluded.